THE DETERMINATION AND NATURE OF THE LYOTROPIC LIQUID CRYSTALLINE PHASE TRANSITIONS IN THE AMMONIUM PENTADECAFLUOROOCTANOATE DEUTERIUM OXIDE SYSTEM.

A thesis presented in partial fulfilment

of the requirements for the degree

of Master of Science

in Chemistry at

Massey University

Mark Hamish Smith

1986

Acknowledgements

I wish to thank my supervisor Dr Ken Jolley for his guidance and assistance and especially for his patience.

I would also like to thank Dr G R Hedwig and Dr P D Buckely for their advice and encouragement.

I thank the glassblower Mr Grant Platt for his cooperation in the rapid sealing of my NMR sample tubes.

I am grateful to Dr A MacGibbon for allowing me to use the DSC at the DRI and for his help in the running of the machine and the interpretation of the results.

I would also like to thank Dr N Boden for his invaluable discussions about the field of lyotropic liquid crystals that took place during his visit in January of 1985.

Finally I would like to thank Tui Totman and Rob Sykes for their assistance in the production of this thesis.

ABSTRACT

The work presented in this thesis is the first stage in an investigation into the role of the counter-ion in determining phase behaviour. Specifically a high resolution phase diagram of the system ammonium pentadecafluorooctanoate/heavy water has been obtained and compared with that of the system caesium pentadecafluorooctanoate/heavy water. Three physical techniques were used, namely; deuterium NMR spectroscopy, differential scanning calorimetry and conductivity measurements. The main method used for phase transition identification was deuterium NMR spectroscopy and therefore a detailed NMR theory section is included.

Experimental evidence indicates no difference in the nature of the mesophases for the different counter-ion systems studied. There is, however, a difference in the temperatures and compositions at which the phase transitions occur in the two systems. These differences are interpreted in terms of differences in the solubilities of the salts and the hydration energies of the counterions.

INTRODUCTION

In 1890,O Lehmann [1] first used the term liquid crystal to descibe the states of matter intermediate to crystalline solid and normal (isotropic) liquid phases, which due to their milky appearance were originally thought of as being impure solutions. Many thousands of organic compounds exhibit liquid crystalline behaviour above their melting points, and these liquid crystals have since been referred to as the fourth state of matter. Liquid crystals fall into two main classes - Thermotropic and Lyotropic.

Thermotropic Liquid Crystals

The name thermotropic derives from the fact that the main factor determining the phase is the temperature. Thermotropics are usually large organic molecules with various functional groups such as azobenzenes,azoxybenzenes,nitrones and numerous others. The vast majority have the structure

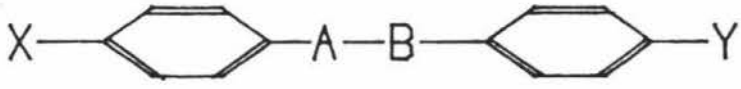

and possess two or more aromatic rings,one or more bridging groups,A-B,that bind the rings together,and two terminal groups X and Y usually on the long axis of the molecule. X and Y are often the same group. An example of a thermotropic liquid crystal is p-azoxybenzene which has the structure.

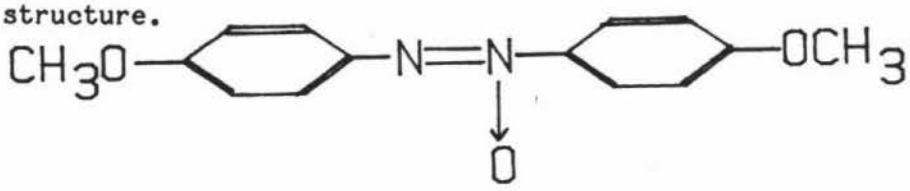

Thermotropics are single component systems or mixtures of similar types of molecules. For example 4-Methoxy-4'-n-butyl-benzylideneaniline (MBBA) is an important room temperature nematic liquid crystal whose liquid crystalline temperature range can be increased by the addition

of 4-ethoxy-4'-n-butyl-benzylideneaniline (EBBA)[2].

There are three basic types of thermotropic liquid crystalline mesophases [3]:smectic,from the Greek for greasy;nematic,from the Greek for threads; and cholesteric so called because it is mostly formed by cholesteryl derivatives (but not cholestertol itself). A schematic representation of the ordering of the symmetry axes of the molecules in each of these phases is given below.

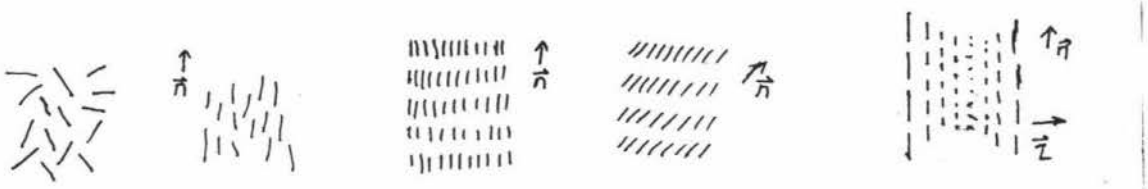

isotropic nematic smectic A smectic C cholesteric

There are many types of smectic liquid crystals that have been given the designation of smectic A,B,C...etc [4]. Smectic liquid crystals have a layered structure with the centres of gravity of the elongated molecules arranged in equidistant planes. The long axes of the molecules are parallel to a prefered direction, known as the director $\vec{n}$,which may be normal to the planes (smectic A) or tilted to a certain angle for example (smectic C).

Nematic liquid crystals have long range orientational order of the long molecular axes but no long range translational order. Nematics are important technologically because they can be aligned such that the orientational order can be extended over the whole of a macroscopic sample by either a magnetic field or an electric field. Use of the latter is made in Liquid Crystal Displays (LCD's). A simple LCD consists of two glass plates coated on the inside surface with a transparent electrode layer between which a liquid crystal has been

sandwiched.

Cholesteric liquid crystalline mesophases can be thought of as being a twisted nematic structure where the molecules are aligned parallel to a prefered direction ,$\vec{n}$. The molecules that make up a cholesteric mesophase are usually flat and lie together in planes. The mesophase is made up of layers of these planes with each of the planes being rotated slightly about an axis perpendicular to the planes. When proceeding normal to the plane $\vec{n}$ rotates continuously giving a helical type structure the axis of which is given by another vector quantity ,$\vec{z}$. The pitch ,P, is the proportion of 2π necessary to rotate $\vec{n}$ when proceeding along $\vec{z}$ or in other words the angle that each plane has been rotated relative to the previous plane. Certain cholesteric liquid crystals exhibit colour changes over the entire colour scale from red to violet when a variable such as temperature is changed. This gives rise to applications such as skin temperature measurement for the diagnosis of tumours and vascular disease and for monitoring skin grafts.

Recently another type of thermotropic phase has been discovered which is made up of flat disc shaped molecules [5]. These molecules have their symmetry axes perpendicular to the plane of each disc and tend to form a hexagonal columnar phases in which the molecules are stacked on top of each other. The sequence of phase transitions is columnar to nematic to isotropic.

Lyotropic Liquid Crystals

Lyotropic liquid crystals are formed on mixing two or more components. One of these components must be an amphiphile,a molecule which contains

a polar head group (usually ionic) and one or more long hydrophobic chains,and one of the other components in the system must be a solvent (usually water). Lyotropic liquid crystals occur in all living systems. Examples of this are cell membranes which are liquid crystals made up of bilayers of phospholipids. Man made lyotropic liquid crystals can be traced as far back as Ancient Rome when a primitive form of soap was used which when mixed with water gave the first artificially produced liquid crystalline mesophase [6]. In spite of this,very little quantitative work has been undertaken on these systems and our knowledge is very primitive.

Most of the work done until fairly recently has been qualitative and has been undertaken on the behalf of soap and detergent manufacturers. This work was not particularly detailed and was aimed at ensuring that the soap remained in an easy to handle low viscosity phase rather than a more troublesome high viscosity phase. Phases were identified and labelled by names such as neat soap,middle soap and isotropic phase.

The dissolution of an amphiphile in water gives micelles at low concentrations and liquid crystals (lyotropic amphiphillic mesophases) at higher ones. Critical micelle concentrations (c.m.c.) are typically 10^{-3} to 10^{-1} mol dm^{-3} whilst `critical' liquid crystal concentrations can be as low as 0.5 mol dm^{-3}. In micellar solutions the amphiphilic aggregates are of finite size (small spheres , rods or discs), whilst in mesophases they have traditionally been envisaged as being of indefinite size (cylinders or bimolecular layers)[7]. For mainly this reason studies of micellar solutions,on the one hand, and mesophases,on the other,have developed into separate domains of

endeavour. The relatively recent discovery of nematic mesophases [8] and the results of subsequent investigations of their structures and properties clearly indicate,however,that our fundamental understanding of liquid crystal mesophases cannot be diverted from that of micellar solutions.

Nematic mesophases are micellar solutions in which there is long range orientational ordering of the symmetry axes of the micelles. Nematic phases consisting of discoid (oblate ellipsoids or discs) micelles (N_D) tend to occur intermediate to lamellar phases and isotropic micellar solutions,whilst ones consisting of calamitic (prolate ellipsoids or rods) micelles (N_C) occur intermediate to hexagonal phases and isotropic micellar solutions [9]. In terms of their symmetry properties, the former can be compared with the thermotropic smectic A to nematic to isotropic liquid sequence of phases exhibited by calamitic molecules and the latter to the thermotropic columnar to nematic to isotropic liquid sequence exhibited by discoid molecules. It is not unreasonable, therefore, to expect that phase transitions in lyotropic systems can be understood in terms of the theories developed for thermotropic systems. But it is not necessarily so because the two kinds of system are fundamentally different from each other in one important aspect. In lyotropic systems the mesogenic particles are amphiphilic aggregates whose detailed structures vary with the thermodynamic state (i.e temperature, pressure, composition, and mesophase structures) whilst in thermotropic systems the structure of the particles is an invariant property (except for internal conformational changes). Phenomenological theories have been developed which attempt to relate the detailed molecular organisation of the

aggregates to the molecular and inter-aggregate interactions, but these are, at best, primitive [10].

The major impediment to the development of applicable models is the paucity of experimental data about the structures of the aggregates in the various mesophases. For example, the conventional opinion is that lamellar phases consist of bimolecular lamellae of indefinite extent separated by layers of water (neglecting macroscopic structural defects) [7]. Yet, it has recently been suggested [11] that, at least in cases where the lamellar phase gives way to a nematic phase with either increasing temperature or on dilution, the lamellae are actually two dimensional arrays of discoid micelles. An alternative proposal [12] is that the lamellae consist of continuous bimolecular layers (bilayers) penetrated by irregularly shaped `pools' of water and that in the conjugate nematic phase the aggregates are irregularly shaped bilayers. The most likely situation which obtains is that the lamellar phase exists with a variety of structural modifications not unlike the polymorphism of the thermotropic smectic liquid crystals. It is also very probable that the lyotropic columnar phases (hexagonal, tetragonal) will exhibit a wide variety of polymorphism. In the case of the nematic mesophases, it is not known what factors control the size and shape of the micelles and under what conditions these mesophases are thermodynamically stable. A significant and unexpected observation in this context is that in the N_D^+ mesophase of the caesium pentadecafluorooctanoate (CsPFO)/water system the dimensions of the micelles are of the order of the separation of their centres-of-mass, irrespective of amphiphile concentration [13].

Clearly there is a need at present for careful experimental studies of the structure of the amphiphilic aggregates and of the basic physics of the phase transformations for well defined systems which exhibit simple sequences of mesophases such as those referred to above. To explore these phenomena we have embarked on detailed studies of lyotropic liquid crystalline systems.

We have chosen as our model the salts of pentadecafluorooctanoic acid in water. The features that make these systems attractive are as follows. Firstly, fluorinated amphiphiles are much more stable, both chemically and thermally, than hydrocarbon ones. Secondly, they are all simple two component systems. Thirdly, in many systems a nematic phase (N_D^+) occurs over a wide range of concentrations and it is intermediate to a lamellar phase and an isotropic micellar solution, and fourthly, they have a positive diamagnetic anisotropy so that samples with a homeotropic distribution of directors can be prepared. The latter property is of special importance for experimental studies. To our knowledge, there is no other system known to date (apart from the salts of pentadecafluorooctanoic acid and their homologues) which satisfy these requirements.

As a first step in these studies it is vital that accurate phase diagrams be produced. The first system to be studied in detail was the CsPFO/D_2O system a partial phase diagram of limited accuracy for which has been published [14]. Subsequent work undertaken at Leeds and Massey Universities has resulted in a considerable improvement in the resolution of this phase diagram [15]. The refined phase diagram for the CsPFO/D_2O system is shown in Figure 1. The ordinate gives the

Figure 1. The complete phase diagram for the CsPFO/D_2O system. C, crystal; L, lamellar phase; N_D^+, nematic phase with positive diamagnetic anisotropy and discoid micelles; I, isotropic micellar solution; HI, heavy ice. Triple points and other points of interest are as labeled.
From Ref. 15.

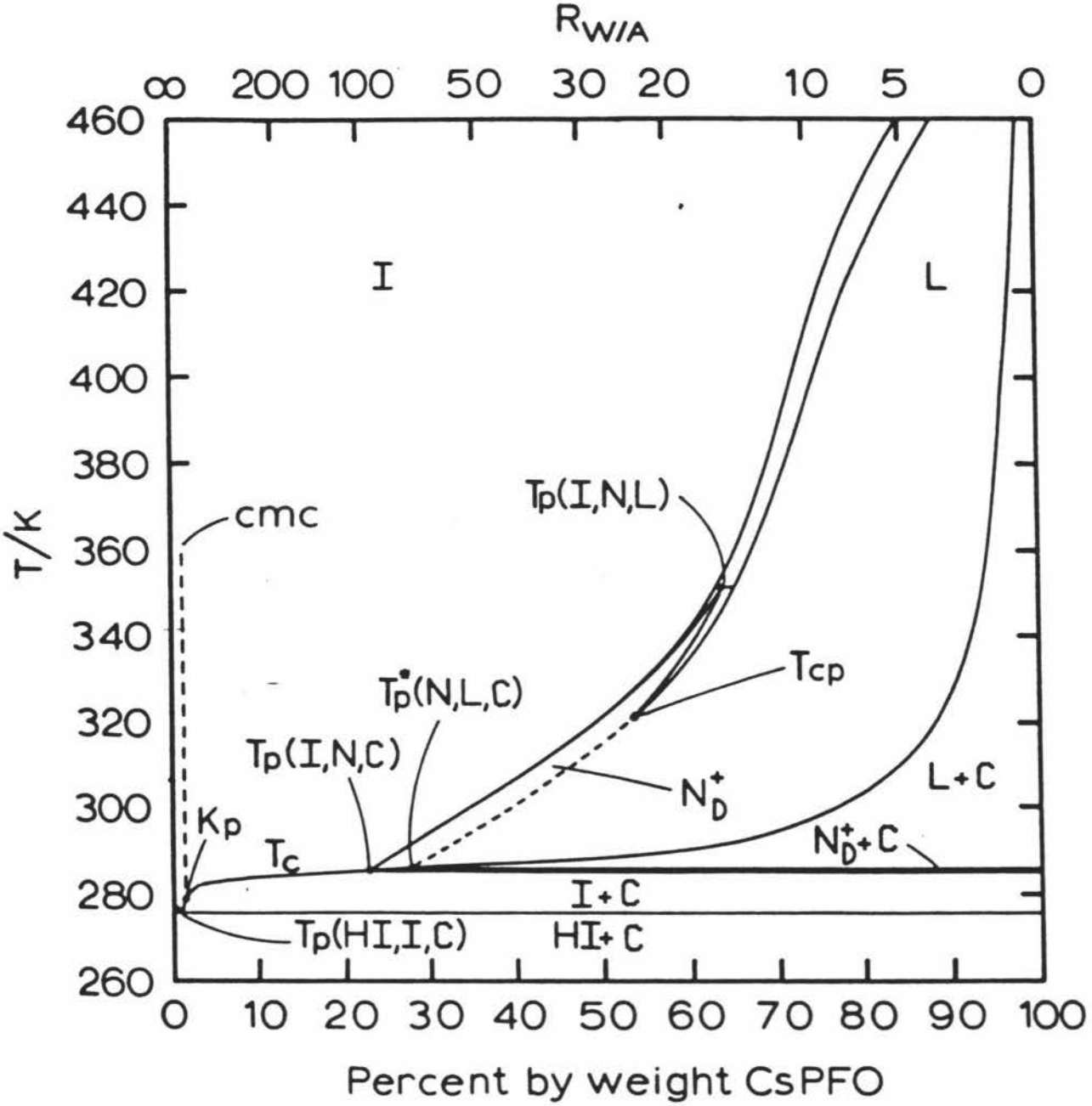
$R_{W/A}$
∞ 200 100 50 30 20 10 5 0
460
440
420
400
380
360
340
320
300
280
260
T/K
I
L
cmc
$T_p(I,N,L)$
$T_p^*(N,L,C)$
T_{cp}
$T_p(I,N,C)$
N_D^+
L+C
K_p
T_c
$N_D^+ + C$
I+C
$T_p(HI,I,C)$
HI+C
0 10 20 30 40 50 60 70 80 90 100
Percent by weight CsPFO

temperature and the abscissa the concentration. The latter is given as the percentage by weight of CsPFO on the lower axis and as the mole ratio of water (D_2O) to CsPFO (amphiphile A) $R_{W/A}$ on the top axis. The diagram is unusually simple when compared with those of other amphiphile/water mixtures and shows a number of unique and interesting features.

There are only three homogeneous single phase regions, apart from the pure compounds. These are the isotropic micellar solution, I, (simple molecular solution of amphiphile in water for concentrations less than c.m.c) the nematic phase, N_D^+, and the lamellar phase, L. All of the other areas are two-phase regions in which the system separates into two phases with compositions given by the intersection of horizontal lines (tie-lines) with the phase boundary curves and proportions given by the lever rule. The crystalline CsPFO (C) and heavy ice (HI) are completely immiscible and there is a triple point (eutectic point) Tp(HI,I,C). The curve Tc is the solubility curve for the crystalline amphiphile. The solubility curve meets the c.m.c line at the Krafft point Kp. At higher concentrations, first nematic, then lamellar mesophases are formed. The lamellar phase is unusual for a simple ionic amphiphile in that it occurs over an unusually wide range of concentration. The nematic phase is intermediate to the lamellar and isotropic micellar solution phases and again we see that it exists over an extensive concentration interval; in fact, this is far greater than in any other amphiphile/water system so far reported. For concentrations of amphiphile less than 53.5 weight percent (the composition of an apparent tricritical point, Tcp) the lamellar to nematic phase transition appears to be continuous (i.e no mixed phase

region) suggesting that these transitions are of a higher order than first. It may however simply represent an inability of ^{2}H NMR to distinguish between first and higher order transitions in this region of the phase diagram. This point will be examined in detail in the NMR section of this thesis. The temperature and composition of the various points on the phase diagram are summarised in Table 1.

Table 1. Location of specific points on the CsPFO/D_2O phase diagram.

Point	wt%Amphiphile	Temperature
Tp(I,N,L)	63.0	351.0 K
Tcp	53.5	322.0 K
Tp(I,N,C)	22.5	285.3 K
Tp(N,L,C)	27.5	285.6 K
Kp	1.0	279.0 K
Tp(HI,I,C)	0.9	276.0 K

The purpose of the work presented in this thesis was to investigate the system ammonium pentadecafluorooctanoate/D_2O (APFO/D_2O) as a first step in an investigation into the role of the counter ion in the determination of liquid crystal phase structure and phase transition mechanisms. This system has all the advantages associated with the CsPFO/D_2O system. Previous studies on heptadecafluorononanoate salts [16] suggest that the phase diagram of the ammonium salt should be similar to that of the caesium salt. This study was of a cursory nature however and although a magnetically orientable phase (nematic phase) was identified for the caesium salt no such phase was recognised for the ammonium salt. Hoffmann [17] has recently reported results on

the ammonium heptadecafluorononanoate/D_2O system where a nematic phase was recognised but not fully characterised. This work was later incorporated in another paper which was concerned with the formation of lyotropic liquid crystal mesophases from micellar solutions [18].

Specifically the aim of this work can be divided into two parts.
(1) To map out a high resolution phase diagram for the APFO/D_2O system.
(2) To compare the APFO/D_2O phase diagram with that for the CsPFO/D_2O phase diagram to see if some insight into the role of the counter ion in determining liquid crystal phase structure and phase transition mechanisms could be found.

Experimental

Materials

Ammonium pentadecafluorooctanoate was prepared by the neutralisation of pentadecafluorooctanoic acid (from Koch-Light and Riedel-De Haen) with ammonium hydroxide. The resulting solution was then freeze dried. The APFO thus obtained was recrystallised from a 1:1 butanol/hexane mixture to remove any unreacted acid and then dried under vacuum. No true melting point was established for APFO because it decomposes at 124-128^{o}C The source of the acid used to make the APFO made no difference to any of the measured phase transition temperatures.

NMR

The NMR samples were made by weighing D_2O (Sigma USA ,99.8% ^{2}H) and the APFO directly into 5mm o.d. NMR tubes which were then flame sealed. To avoid losses when the tube is sealed the salt is introduced into the base of the tube through a long glass funnel and the D_2O is added through a long hypodermic syringe needle. The tubes after sealing were placed in an oven at 80^{o}C to equilibrate and were left until they appeared homogeneous.

DSC

For DSC measurements samples were made up into sealed glass vials in the same way as the samples used for NMR. These samples were broken just prior to use then weighed into aluminium pans which were sealed by having their lids crimped in a small press.

Conductivity

A range of weight percent samples from 0.3 to 15 wt% amphiphile were made up by weighing out of a stock 15 wt% amphiphile solution.

Measurements

NMR

Deuterium spectra of D_2O were obtained using a JEOL FX-60 pulse fourier transform NMR. The probe used was originally from a JEOL FX-100. The ^{13}C observation coil of this probe was retuned from 25MHz to the deuterium observation frequency of 9.18MHz. The output signal from this coil was fed into the deuterium lock preamlifier of the probe which was retuned from 15MHz to 9.18MHz. The deuterium lock channel was then used as the observe channel by switching over the lock and observe amplifiers and oscillators on the spectrometer. Field frequency stability was achieved by using an external proton lock (built by C Eccles,Massey). The retuning resulted in a large decrease in the "Q" of the coil and a consequent long $\pi/2$ pulse time of 250 μs. Usually $\pi/4$ pulses were used giving an effective frequency spread of $\pm$2000Hz from the observation pulse frequency which was greater than the range of deuterium frequencies measured in this study. Typically ten repetitions of the $\pi/4$ pulse at 2s intervals were required to produce an adequate signal to noise ratio in the FID. Data were subsequently Fourier transformed using 4000 data points. Sweep widths of 1000Hz were usually used. The temperature control for the system was achieved using a double pass water flow cell (Fig 2) (designed at Leeds University) connected to a Colora WK3 cryostat. This provides temperature control to a precision of $\pm$5 mK.

DSC

The DSC measurements were made using a Perkin-Elmer DSC-2 instrument interfaced with a model 3600 thermal analysis data station which belongs to the Dairy Research Institute, Palmerston North. The DSC was temperature calibrated using a standard indium sample. A schematic

Figure 2. The double pass water flow system used in the NMR experiments.

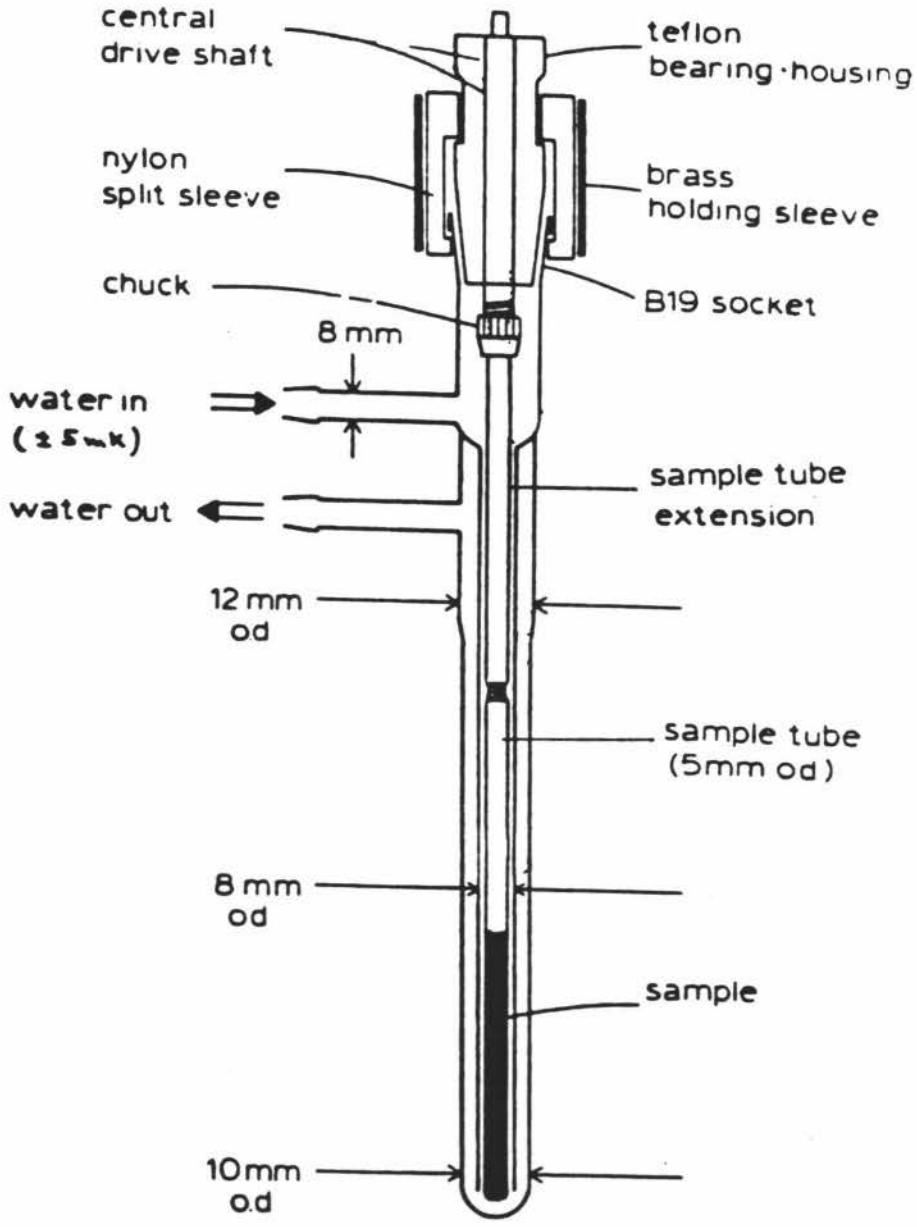
central
drive shaft
teflon
bearing housing
nylon
split sleeve
brass
holding sleeve
chuck
B19 socket
8 mm
water in
(±5mk)
water out
sample tube
extension
12 mm
od
sample tube
(5mm od)
8 mm
od
sample
10mm
o.d

diagram of the instrument is given below.

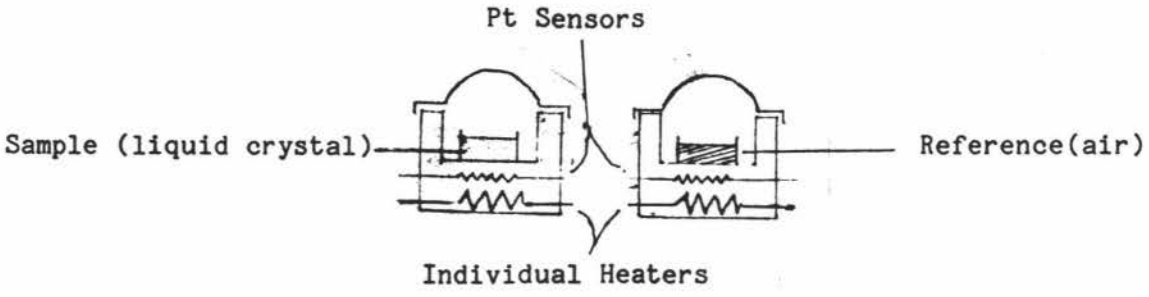

The DSC can be thought of as having two control loops.

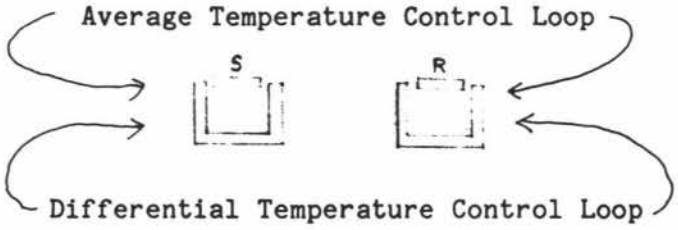

The average temperature control loop enables the temperature of the sample and reference to be increased (or decreased) at a specified rate. The second loop ensures that if a temperature difference develops between the sample and reference , because of an exothermic or endothermic reaction in the sample , the power imput is adjusted to remove this difference. This is known as the null-balance principle. This means that the temperature of the sample holder is always kept the same as that of the reference holder by continuous and automatic adjustment of the heater power. A signal proportional to the difference between the heater input to the sample and that of the reference, dH/dt, is fed into the computer for subsequent analysis.

Conductivity

Conductivity measurements were made using a Phillips PW9509 digital

conductivity meter attached to a Phillips PW9512/61 conductivity cell. A KCl sample of known molality was used to determine the cell constant. The conductivity meter was operated at a frequency of 2000Hz. To regulate the temperature of the sample a double pass water flow system was attached to the outside of the cell (Fig 3) and the Colora Wk3 cryostat was used to control the water temperature to a precisions of $\pm$5 mK , the same as for the NMR experiments.

Temperature

All of the temperature measurements for the NMR and conductivity experiments were made using a thermister connected to a Fluke 8050A digital multimeter. The thermister was calibrated against a Hewlett-Packard 2801A digital quartz thermometer coupled with a 2850A temperature probe which had been calibrated at the Physics and Engineering Laboratory of the DSIR in Wellington to an accuracy of 1 mK. The response of the thermister resistance to temperature was accurately represented over small temperature ranges by an Arrhenius expression

$$R = Ae^{B/T}$$

The calibration data was fitted to the above equation and a linear regression performed for the best fit A and B values. The regression coefficients (given in the following table) were then incorporated into a computer program written for the Hewlett-Packard HP85 desk-top computer which calculated the thermodynamic temperature corresponding to any given resistance reading within the calibration range.

Figure 3. The double pass water flow system used in the conductivity experiments.

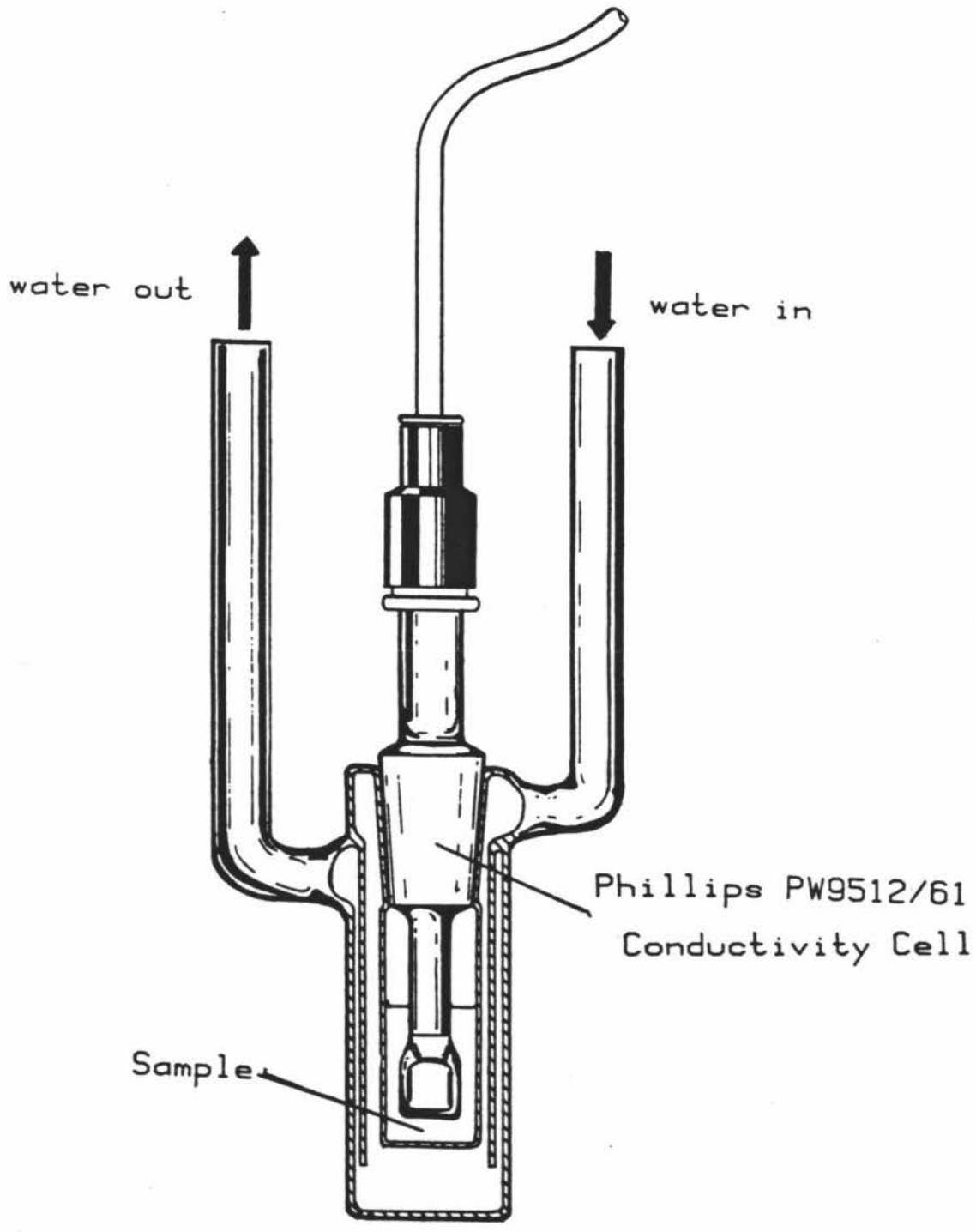
water out
water in
Phillips PW9512/61
Conductivity Cell
Sample

Calibration Coefficients

T range/K	$Ax10^{5}/k\Omega$	$Bx10^{-3}/K$	r^2
278-293	8.06559	3.11194	0.999996
293-309	7.30319	3.14105	0.999997
309-327	6.80805	3.16291	1.000000
327-348	6.63824	3.17112	0.999999
348-360	6.54938	3.17593	0.999996

r is the coefficient of linear correlation.

The accuracy of the temperatures so measured is $\pm$0.01 K. The high flow rate of the water meant that the temperature of the water entering the sample cell was the same as that leaving the cell within measurement error and therefore ,as expected, it made no difference to the temperature reading if the thermister was in the cell outlet or the cell inlet. This also indicates that the sample resides in a uniform temperature enclosure in which for all practical purposes temperature gradients are absent.

NMR Theory

NMR measurements of the quadrupole splitting of ^2H in labelled water is an unparalleled method for mapping phase diagrams and for studying the mechanism of phase transitions in lyotropic amphiphilic liquid crystals. This is because the quadrupole splitting is a characteristic signature of each kind of phase and is also a function of composition and temperature. It can, therefore, provide detailed information about the uniformity of composition and temperature in bulk samples. This is particularly useful information when traversing two-phase regions as in most instances it enables both the compositions and the relative amounts of the coexisting phases to be monitored. It can also be used to monitor the orientational distribution of the mesophase director in the sample under study and to distinguish between uniaxial and biaxial mesophases. For this reason the NMR theory will be presented in some detail.

The spectrum for ^2H spins (I=1) in labelled water in a macroscopically aligned uniaxial mesophase (nematic , lamellar or hexagonal) is always a symmetric doublet whose quadrupole splitting $\Delta\tilde{\nu}$ is given by

$$\Delta\tilde{\nu} = 3/2\ |\tilde{q}_{zz}|\bar{p}_2 p_2(\cos\Phi) \quad (1)$$

$p_2(\cos\Phi) = 1/3(3\cos^2\Phi - 1)$ where is the angle between the mesophase director $\vec{n}$ and the direction of the magnetic field $\vec{B}$ and $\tilde{q}_{zz}$ is the partially averaged component of the deuterium nuclear quadrupole-electric field coupling measured parallel to the director.

$$\tilde{q}_{zz} = \Sigma p_n \chi_n \{S^n_{cc} + \eta_n(S^n_{aa} - S^n_{bb})\} \quad (2)$$

The S^n_{ij} are the elements of the Saupe ordering matrix for the principle axes (a,b,c) of the nuclear quadrupole coupling interaction tensor at the nth site with statistical weight p_n . $\chi_n = (e^2qQ/h)n$ is the

quadrupole coupling constant and η_n is the assymetry parameter. Since for unbound water molecules $\tilde{q}_{zz}$ is zero we have,

$$|\tilde{q}_{zz}| = \frac{n_b x_a}{x_{D_2O}} |\tilde{q}_{zz}|_b \qquad (3)$$

where n_b is the number of water molecules "bound" at the aggregate/water interface (unknown but small) and x_a and x_{D_2O} are the mole fractions of amphiphile and water respectively. $\bar{P}_2$ is a second rank order parameter defined for a monodisperse assembly of micelles by

$$\bar{P}_2 = (3\langle\cos^2\beta\rangle - 1)/2 \qquad (4)$$

where β is the angle between the symmetry axis of the structural units ($\vec{m}$) and the mesophase director ($\vec{n}$) and the angular brackets indicate an ensemble average. For any pure liquid crystal phase $\bar{P}_2$ increases as the temperature decreases as a consquence of the increasing order within the system. A diagramatical representation of the relationship between the vector quantities refered to above, is given in the following figure.

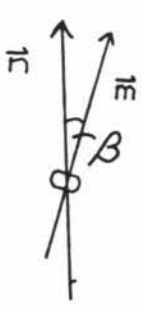

$\bar{P}_2$ will be zero for an isotropic micellar solution and therefore a singlet spectrum is the result. For a nematic mesophase or a lamellar mesophase consisting of two dimensional arrays of discrete discoidal micelles, $0 < \bar{P}_2 < 1$, whereas for the classical lamellar mesophase consisting of infinite bilayers , $\bar{P}_2$ must be equal to one. Both of these lamellar phases will give rise to a doublet spectrum as will the nematic mesophase. The observation of a single doublet implies that motions of the water molecules are fast compared to the experimental time length. The nematic and lamellar mesophases can be distinguished

by their responses to the altering of the position of the mesophase director relative to the spectrometer magnetic field, $\vec{B}$. The nematic mesophase has a finite rotational viscosity coefficient and positive diamagnetic anisotropy and the mesophase director, $\vec{n}$, aligns itself with the magnetic field, $\vec{B}$. Following rotation the sample will realign itself so that its mesophase director, $\vec{n}$, again lies along the direction of the magnetic field , $\vec{B}$. This reorientation takes place in the order of a few seconds over most of the nematic range. and once reorientation is complete and all directors are aligned with $\vec{B}$, a single sharp doublet is again observed. The lamellar phase has a rotational viscosity coefficient of infinite value and therefore the lamellar director is locked into the mesophase and cannot reorientate along $\vec{B}$. After being rotated the spectrum is still a well defined doublet whose splitting is defined by equation (1), i.e $\Delta\tilde{\nu}$ follows a $3\cos^2\Phi-1$ angular dependence. A different spectrum for the lamellar phase is obtained if the sample is cooled outside the magnet instead of inside it. The sample cooled outside the magnet gives a `Pake' spectrum which is consistent with an isotropic director distribution (Fig 4).

The above description refers to a homogeneous (single phase) situation. When two phases are present complications are introduced due to exchange of the D_2O between the phases. For example in a lamellar/nematic mixed phase sample (both doublets) the observation of separate lamellar and nematic doublets is dependent upon the average time a water molecule spends in a particular phase (τ) and the difference in the quadrupole splitting of the two phases ($\delta\Delta\tilde{\nu}$). The doublets will merge when $\tau \approx 1/\pi\delta\Delta\tilde{\nu}$ so that fast exchange (only one

Figure 4. Deuterium NMR spectra of D_2O in the lamellar phase of a 54.21 wt% APFO/D_2O sample with
(a) a homeotropic distrubution of lamellar directors (normals to the planes of the lamellae) and
(b) an isotropic distribution of directors.

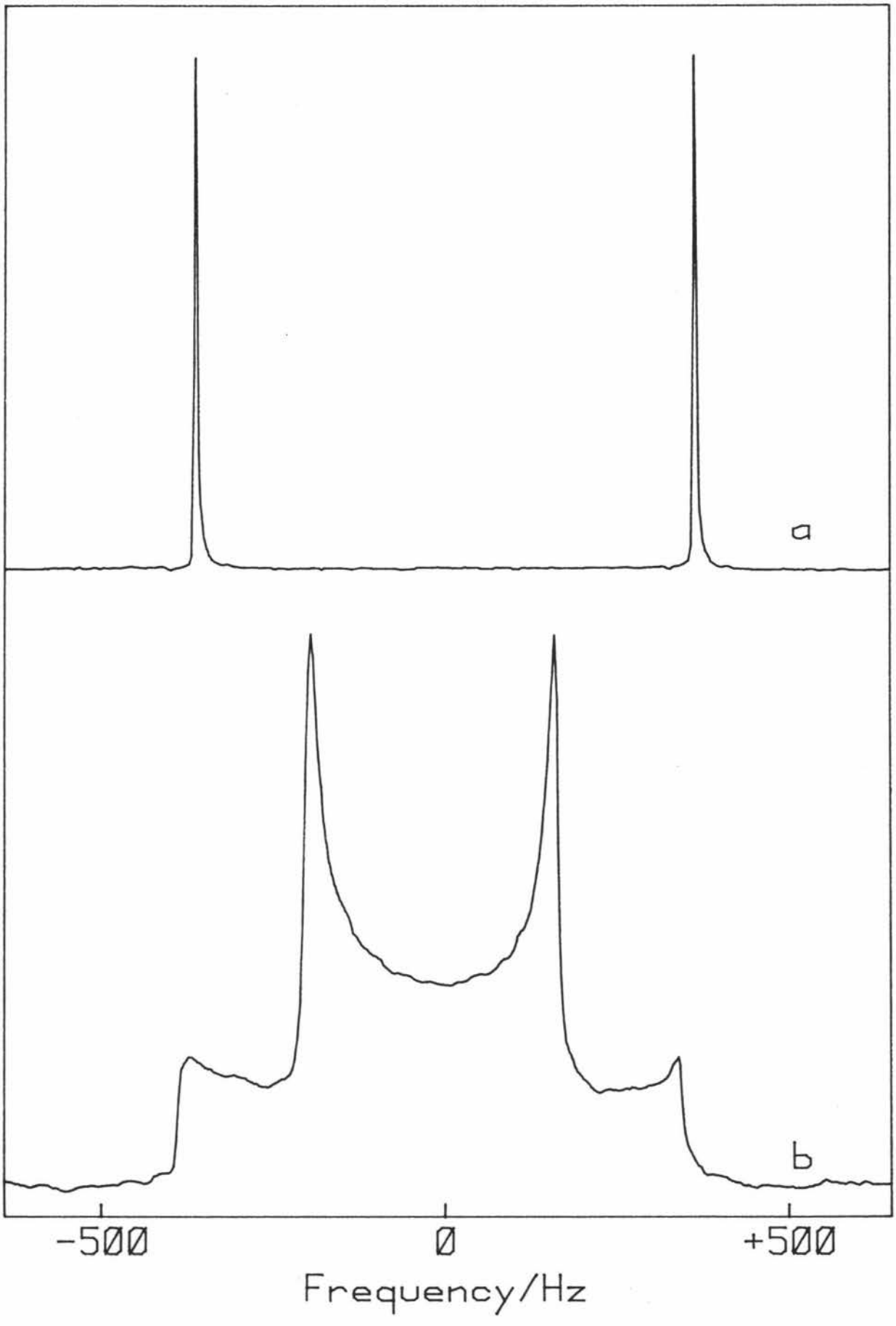
a
b
-500
0
+500
Frequency/Hz

doublet which is a weighted average of the nematic and lamellar doublets) implies $\tau < 1/\pi\delta\tilde{\Delta\nu}$ and conversely $\tau > 1/\pi\delta\tilde{\Delta\nu}$ for slow exchange (where the doublets are resolved).

In the case where the mixed phase consists of isotropic (singlet) and either nematic or lamellar (doublets) the fast exchange condition becomes $\tau < 1/(2\pi\tilde{\Delta\nu})$ where $\tilde{\Delta\nu}$ is the quadrupole splitting of the ^{2}H nucleus of the water in the nematic or lamellar phase domains. In intermediate exchange regions ($\tau \approx 1/(2\pi\tilde{\Delta\nu})$ line broadening will occur. Thus by deuterium NMR we have a means of identifying phases (isotropic, nematic, lamellar) and in favourable situations we can expect to identify mixed phase regions (separate mesophase spectra obtained) and thus in conjunction with the precise and accurate temperature control high resolution phase diagrams can be produced.

Results

The phase diagram for the APFO/D_2O system is given in Fig 5. The ordinate gives the temperature and the abscissa the concentration as weight percent APFO. The ammonium pentadecafluorooctanoate/D_2O system shows an extensive nematic phase over a large range of compositions and temperatures. The nematic phase exists between compositions of 39.6 wt% and 59.6 wt% amphiphile and the temperatures of 291.0 K and 338.4 K. The nematic phase exists up to the isotropic/nematic/lamellar triple point Tp(I,N,L), which occurs at a temperature of 338.4 K. Because the phase transitions in the region of Tp(I,N,L) take place by way of a first order phase transition mechanism the triple point is not a single point but rather a row of points stretching from the isotropic phase boundary to the lamellar phase boundary at the triple point temperature. There is an apparent tricritical point ,Tcp, at an amphiphile composition of 50.8 wt% and at a temperature of 307.2 K. This point is the result of an apparent change from a first order phase transition mechanism to that of a second order mechanism for the lamellar to nematic transition. There is some doubt about the position and even the existence of Tcp and therefore the nematic/lamellar phase boundary between Tcp and the nematic/lamellar/crystalline triple point Tp(N,L,C) is shown on the phase diagram as a dotted line. Tp(N,L,C) is a triple point at which the nematic and lamellar phases exist in the presence of crystalline amphiphile. This fixed point is located at an amphiphile composition of 43.7 wt% and at a temperature of 291.6 K. The other triple point Tp(I,N,C) is located at the position where the isotropic/nematic mixed phase region crosses the solubility curve. Since Tp(I,N,C) is where the three phases coexist ,Tp(I,N,C) is by definition not a single point but a line of points. This line of

Figure 5. A partial phase diagram for the APFO/D_2O system. The symbols used are the same as those used in Fig 1.

The nematic/lamellar transition below Tcp is shown as a dotted line because of uncertainty about the nature of the transition.

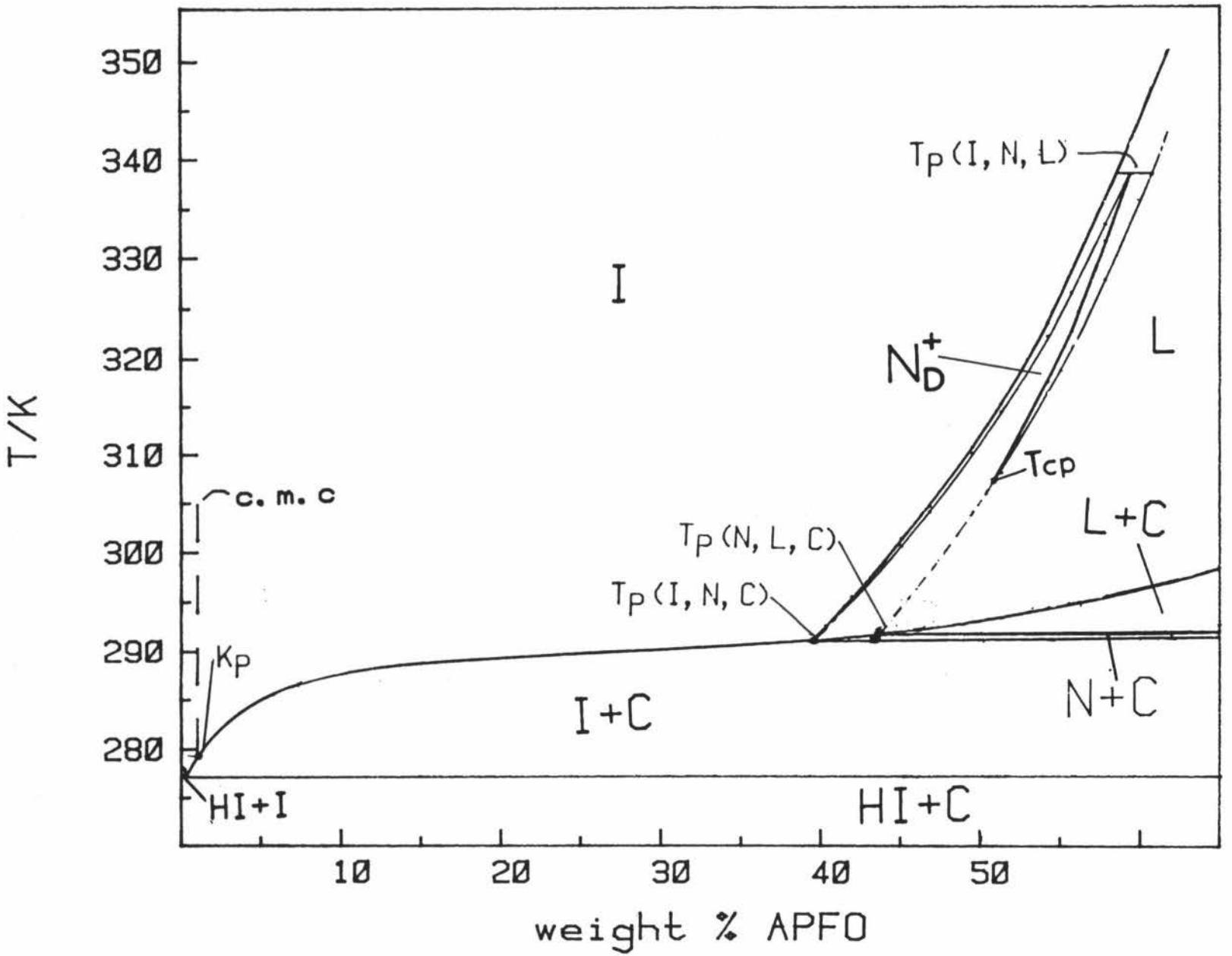
350
340
330
320
310
300
290
280
T/K
I
L
N_D^+
T_P (I, N, L)
T_{cp}
c. m. c
T_P (N, L, C)
T_P (I, N, C)
L+C
K_P
I+C
N+C
HI+I
HI+C
10
20
30
40
50
weight % APFO

points lies on the solubility curve and within the isotropic/nematic mixed phase region. Tp(I,N,C) is therefore located at a temperature of 291.0 K and at a range of compositions between 39.5 wt% and 39.7 wt% amphiphile. The location of the triple points Tp(I,N,C) and Tp(N,L,C) was facilitated by the fact that the APFO/D_2O system (and the CsPFO/D_2O system) produces supercooled liquid crystal mesophases and so the T_{IN},T_{NI} and T_{NL} curves could be extended below Tc. The intersection of these curves with Tc gave the location of the triple points. Another unique point in this system is the eutectic point. At this point the solution and both solid phases coexist i.e. heavy ice, crystal and isotropic solution. This eutectic point occurs at a temperature of 277.0 K and at a composition of 0.4 wt%. The Krafft point occurs at a concentration of 1.1 wt% and a temperature of 279.2 K. The Krafft point is the point where the c.m.c intersects the solubility curve. To the left of the c.m.c curve the isotropic solution is molecular and to the right of it the solution is isotropic micellar.

All the phases have been marked out by using experimental data except for the nematic/crystalline region. This region is intuitive and has been included because the positioning of the Tp(I,N,C) and Tp(N,L,C) triple points at slightly different temperatures demands the inclusion of a nematic/crystalline region. If these triple points were at the same temperature it would imply that all four phases coexisted ,which is not possible and therefore to prevent the meeting of the four phases a narrow nematic/lamellar region is postulated. The temperature and composition of the various points on the APFO/D_2O phase diagram are summarised in Table 2.

Table 2. Location of specific points on the AFFO/D_2O phase diagram

Point	wt%Amphiphile	Temperature
Tp(I,N,L)	59.6	338.4 K
Tcp	50.8	307.1 K
Tp(I,N,C)	39.6	291.0 K
Tp(N,L,C)	43.7	291.6 K
Kp	1.1	279.2 K
Tp(HI,I,C)	0.4	277.0 K

NMR

The phase boundaries T_{IN} ,T_{NI} ,T_{NL} ,T_{LN} ,T_{IL} and T_{LI} have all been determined by deuterium NMR and are defined as follows

T_{IN} - The upper limit of the isotropic/nematic mixed phase region

T_{NI} - The lower limit of the isotropic/nematic mixed phase region

T_{NL} - The upper limit of the nematic/lamellar mixed phase region

T_{LN} - The lower limit of the nematic/lamellar mixed phase region

T_{IL} - The upper limit of the isotropic/lamellar mixed phase region

T_{LI} - The lower limit of the isotropic/lamellar mixed phase region

Before discussing the detailed NMR observations on crossing phase transition boundaries it is instructive to consider the temperature dependence of the quadrupole splitting ($\Delta\tilde{\nu}$) on passing from isotropic to lamellar phase via the nematic phase. There are two types of $\Delta\tilde{\nu}/T$ curves depending on the amphiphile composition. At compositions greater that 51 wt percent APFO separate nematic and lamellar doublets are observed on crossing the nematic/lamellar mixed phase region, whilst below this composition only one doublet is seen. The high amphiphile composition behaviour is illustrated by the 54.21 wt percent

APFO sample as shown in Fig 6.

In the isotropic phase $\tilde{\Delta\nu}$ is equal to zero therefore the spectrum is a singlet. On cooling along the 54.21 wt% isopleth, once T_{IN} is reached a doublet starts to form (as the nematic phase forms $\bar{P}_2>0$, eq 1) and on further cooling the doublet intensity increases at the expense of the intensity of the singlet. The change in the relative amounts of the two phases within the mixed N/I region is consistent with the lever rule and the composition of the two phases can be read from the phase diagram using a horizontal line which intersects the sample composition and the sample temperature. The quadrupole splitting remains constant (to a first approximation) as the temperature is decreased through the mixed phase region due to a fortuitous balancing of temperature effects on $\bar{P}_2$ and $|\tilde{q}_{zz}|$ (equation 1). As the temperature is decreased $\bar{P}_2$ increases and this is balanced by the decrease in $|\tilde{q}_{zz}|$ (eq.3) as a result of the decreasing amphiphile composition of the nematic phase. There is an increase in $\tilde{\Delta\nu}$ as the cooling continues through the pure nematic phase as a consequence of the increase in $\bar{P}_2$. At T_{NL} a discontinuity in $\tilde{\Delta\nu}$ occurs which is accompanied by the appearance of separate nematic and lamellar doublets. This is because within the mixed N/L phase region there is a difference in both $\bar{P}_2$ and $|\tilde{q}_{zz}|$ between the nematic and lamellar phases. These differences are small for the systems we have studied and therefore we can assume that there is no fundamental change in micelle structure as the phase change occurs. The $\tilde{\Delta\nu}$ values for the nematic and lamellar doublets are again fairly constant across the N/L mixed phase region for the same reasons as for the isotropic/nematic mixed phase region. In the lamellar phase $\tilde{\Delta\nu}$ gradually increases with decreasing temperature because of the

Figure 6. Partially averaged quadrupole splitting of D_2O as observed on cooling through the isotropic to nematic and nematic to lamellar transitions in a 54.21 wt% APFO/D_2O sample. Identical behaviour is observed on heating from the ordered lamellar phase to the isotropic micellar phase. Note that the splitting changes discontinuously at the lamellar to nematic transition where it is first order.

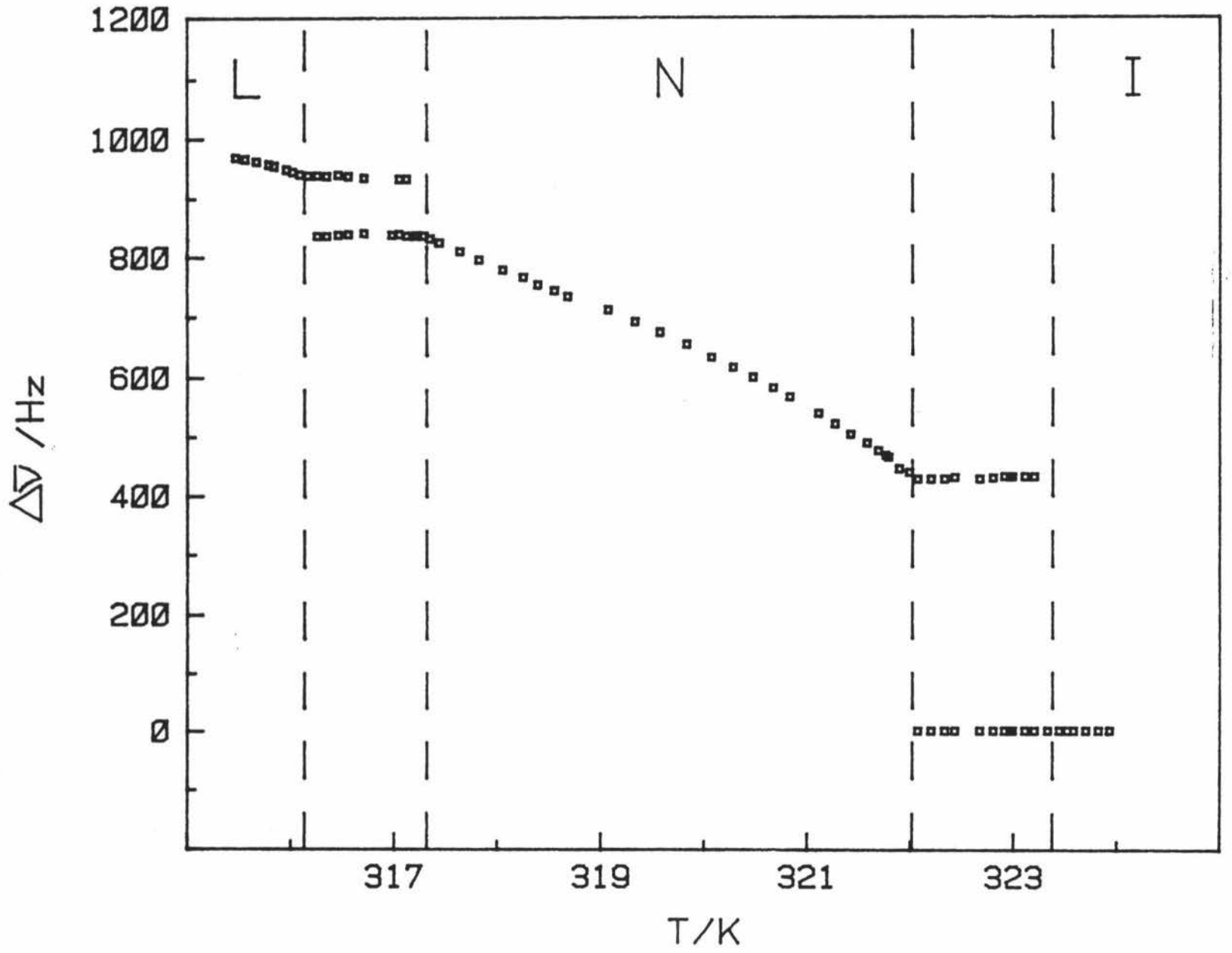
1200
1000
800
600
400
200
0
Δν /Hz
L
N
I
317
319
321
323
T/K

gradual increase in $\bar{p}_2$.

For compositions below Tcp no discontinuity occurs in $\Delta\tilde{\nu}$ but a discontinuity in the temperature dependence of $\Delta\tilde{\nu}$ does occur (Fig 7).

Figure 7. Partially averaged quadrupole splitting of D_2O as observed on cooling through the isotropic to nematic and nematic to lamellar transitions in a 49.50 wt% APFO/D_2O sample. Identical behaviour is observed on heating from the ordered lamellar phase to the isotropic micellar phase. Note that the splitting is continuous across the lamellar to nematic transition but that there is a discontinuity in the temperature dependence of splitting. This is due either to the transition being second order or to it being weakly first order.

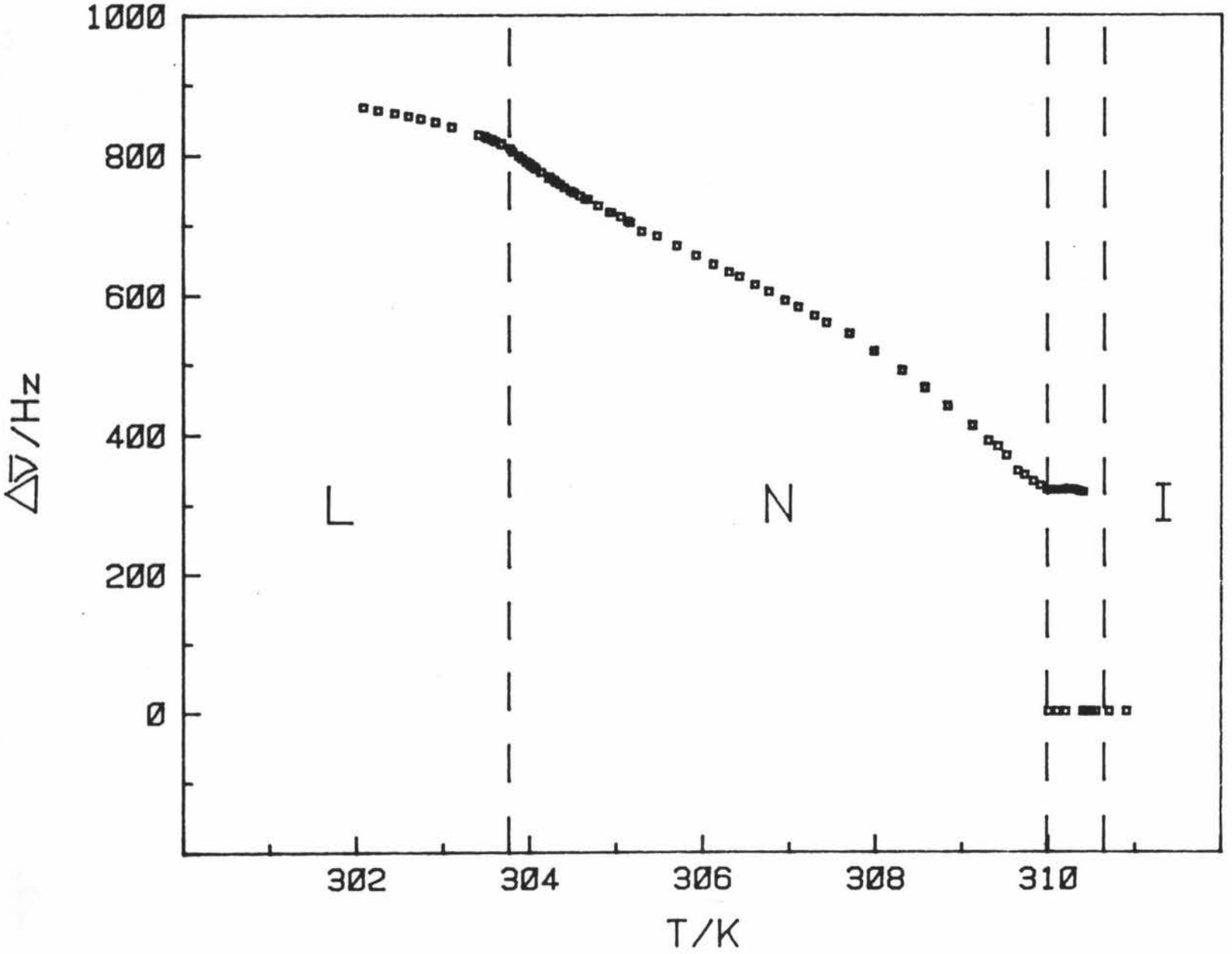
1000
800
600
400
200
0
Δν̄/Hz
L
N
I
302
304
306
308
310
T/K

Determining Phase Boundaries.

Isotropic/nematic mixed phase region.

T_{IN}

The spectra observed when a solution is cooled along isopleth A of Fig 8 are shown in Fig 9. These spectra are of the CsPFO/D_2O system and were obtained at Massey. They illustrate the behaviour of both the CsPFO and APFO/D_2O systems. It is essential to ensure that the sample is throughly mixed in the isotropic phase before it is loaded into the cryostat. The temperature is first adjusted to a temperature about 0.5 K above the nematic/isotropic transition temperature where the spectrum is a singlet since $\bar{P}_2=0$ (eq.1). The sample is then agitated to ensure homogeneity of composition. On slowly cooling (at about 100 mK/min) from the isotropic micellar solution into the isotropic/nematic mixed phase region a symmetrical doublet from the D_2O molecules in the nematic phase is superimposed on the isotropic singlet from the D_2O molecules in the isotropic micellar phase. As cooling continues through the mixed phase region the doublet intensity increases at the expense of the singlet consistent with a variation in the relative amounts of the two phases as described by the lever rule. At the temperature which is the mid-point of the transition the relative intensities of the two spectra are approximately equal (Fig 9b). On further cooling the singlet disappears and the nematic phase is characterised by a single doublet spectrum. When the tube containing the nematic phase sample is spun about its axis which is aligned perpendicular to the direction of the field B at an angular velocity (0.25 Hz) which is much greater than the critical value Ω_c ($\Omega_c=\chi_a B^2/2\mu_o\lambda_1$, where λ_1 is the rotational viscosity coefficient of the nematic phase and χ_a is the anisotropy of the diamagnetic

Figure 8. Portion of the phase diagram of the CsPFO/D_2O system showing the isopleths A,B, and C refered to respectively in Figures 9 and 12 and in the Tp (I,N,L) section of the text (p34).
From Ref. 15

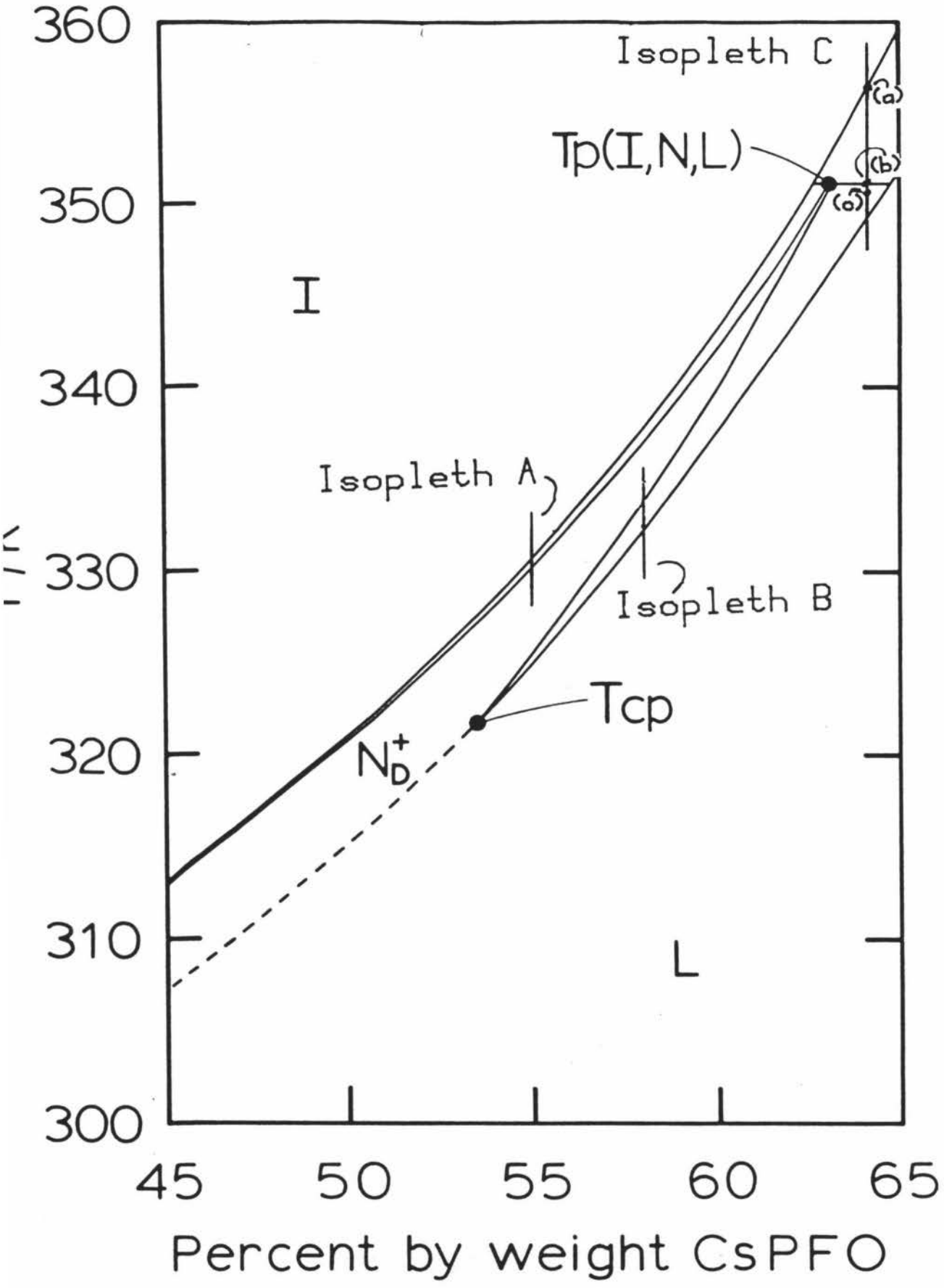
360
350
340
330
320
310
300
45
50
55
60
65
Isopleth C
Tp(I,N,L)
(a)
(b)
(c)
I
Isopleth A
Isopleth B
Tcp
N_D^+
L
Percent by weight CsPFO

Figure 9. Deuterium NMR spectra of D_2O for a 55 wt% CsPFO/D_2O obtained on cooling along isopleth A of Figure 8:

(a) isotropic phase,

(b) nematic/isotropic two phase coexistence region,

(c) nematic phase,

(d) nematic phase rotating at 0.25 Hz about an axis perpendicular to the direction of the magnetic field.

From Ref. 15

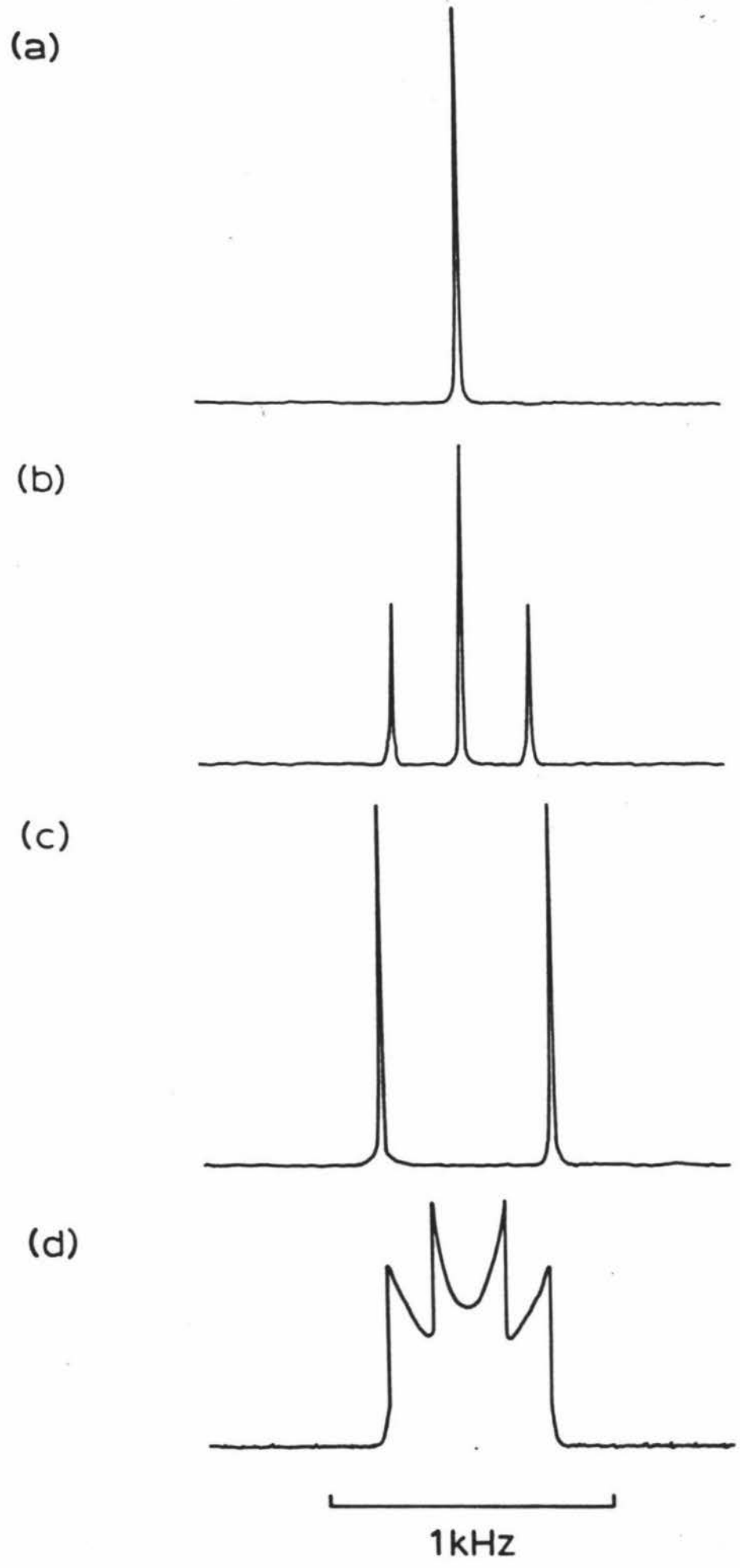
(a)
(b)
(c)
(d)
1kHz

susceptibility) the spectrum shown in Figure 9d is observed. This spectrum corresponds to a two dimensional (planar) distribution of nematic directors in a plane perpendicular to the axis of rotation and confirms that the mesophase has positive diamagnetic anisotropy. When the spinning is stopped the spectrum relaxes quickly to a single doublet. For a mesophase with negative diamagnetic anisotropy a sample with a homeotropic distribution of directors parallel to the axis of rotation would have been obtained and this would have given a single doublet spectrum with one half of the $\Phi=0$ splitting which would not alter when the sample was rotated.

In a homogeneous sample each component of the spectrum is Lorentzian with a width at half height typically of 5Hz. Departures from this simple spectrum are indicative of inhomogeneities in the sample. These inhomogeneities arise from distributions of composition rather than temperature which is maintained uniform over the sample volume. Distributions in composition can arise in two ways. Firstly, by traversing first order transitions in an irreversible manner by changing the temperature too rapidly which can cause either line broadening or a distribution of doublets. Secondly, a concentration gradient can be established along the axis of the sample tube by evaporation of water from the solution, condensation as a film onto the walls of the container and thence back into the solution. This process will occur within a uniform temperature enclosure and can only be suppressed by elimination of the vapour space. But we prefer to have a space above the sample so that it can be easily remixed if and when composition inhomogeneities are introduced on transversing the two phase coexistence regions. Gradients of concentration along the axis

of the tube give rise to a broadening of the spectral lines but this can readily be distinguished from a broadening due to local composition inhomogeneities by applying a magnetic field gradient along the axis of the tube. The former gives rise to an asymmetric spectrum whilst in the case of the latter, both components of the doublet are equally affected.

T_{IN} theoretically should be associated with the first appearance of the nematic doublet on cooling from the pure isotropic phase. The temperature at which this occurs however has been found to be approximately 100 mK lower than the actual T_{IN} value. Experimentally a broadening of the isotropic singlet occurs prior to the appearance of the nematic doublet. The reason for this broadening is chemical exchange between the isotropic and nematic mesophases. On cooling to T_{IN} nematic phase is formed as a microemulsion of nematic domains dispersed in the isotropic continuous phase. The average length of time a D_2O molecule spends in the nematic domains is insufficient for a separate nematic doublet to be observed and the result is broadening of the isotropic singlet. It is the onset of broadening which defines T_{IN} and not the first appearance of the nematic doublet as had previously been assumed [14]. Consideration of the intermediate exchange condition (broadening)

$$\text{i.e.} \quad \tau \approx 1/(2\pi\tilde{\Delta\nu})$$

gives a clue as to the average size of these nematic domains when they are formed. A lower limit is obtained by considering the 57.87 wt% APFO sample in which the quadrupole splitting in the mixed nematic/isotropic phase is ≈580Hz which gives an average nematic domain residence time (τ) of 2.7×10^{-4}s. During this time a D_2O molecule will

undergo a r.m.s displacement of $(2D\tau)^{1/2}$ in any given direction. Taking D, the self diffusion coefficient of D_2O, as $10^{-9}m^2s^{-1}$ gives a displacement of 740nm and so the average diameter of the nematic domains will be of this order when they are first formed. On further cooling the domain sizes increase until the slow exchange condition is realised, at which point separate isotropic and nematic signals are observed.

One way of determining the onset of the broadening is to plot the peak height of the isotropic singlet versus temperature where the onset of broadening is shown by a sharp drop in peak height. However it has been found to be much more simple to observe the FID as the temperature is lowered. The line broadening can easily be determined by a shortening of the time constant of the FID (Fig 10). This method is reproducible and reversible and the transition temperature can be determined to within 10 mK ,which is the accuracy of our temperature control system. This system also has the advantage of being very fast. The reason for this is that the spectrometer can be run in the real time mode. The sample can be rapidly cooled until the time constant for the FID shortens and then heated slightly and cooled slowly through the transition.

T_{NI}

The best method for determining T_{NI} is to plot $\Delta\tilde{\nu}$ versus temperature. T_{NI} is the intersection of the $\Delta\tilde{\nu}/T$ curve for the nematic with that of the mixed phase region as shown in Figure 11. Theoretically the appearance of the singlet on heating could be used to determine T_{NI} but exchange caused by the small size of the isotropic domains gives rise to an incorrect phase transition temperature. The domain sizes are too

Figure 10. Free Induction Decays (FID) for a sample in the isotropic phase (upper) and on just entering the isotropic/nematic mixed phase region (lower). The onset of D_2O exchange between the two phases is clearly revealed by a shortening in the time constant of the FID.

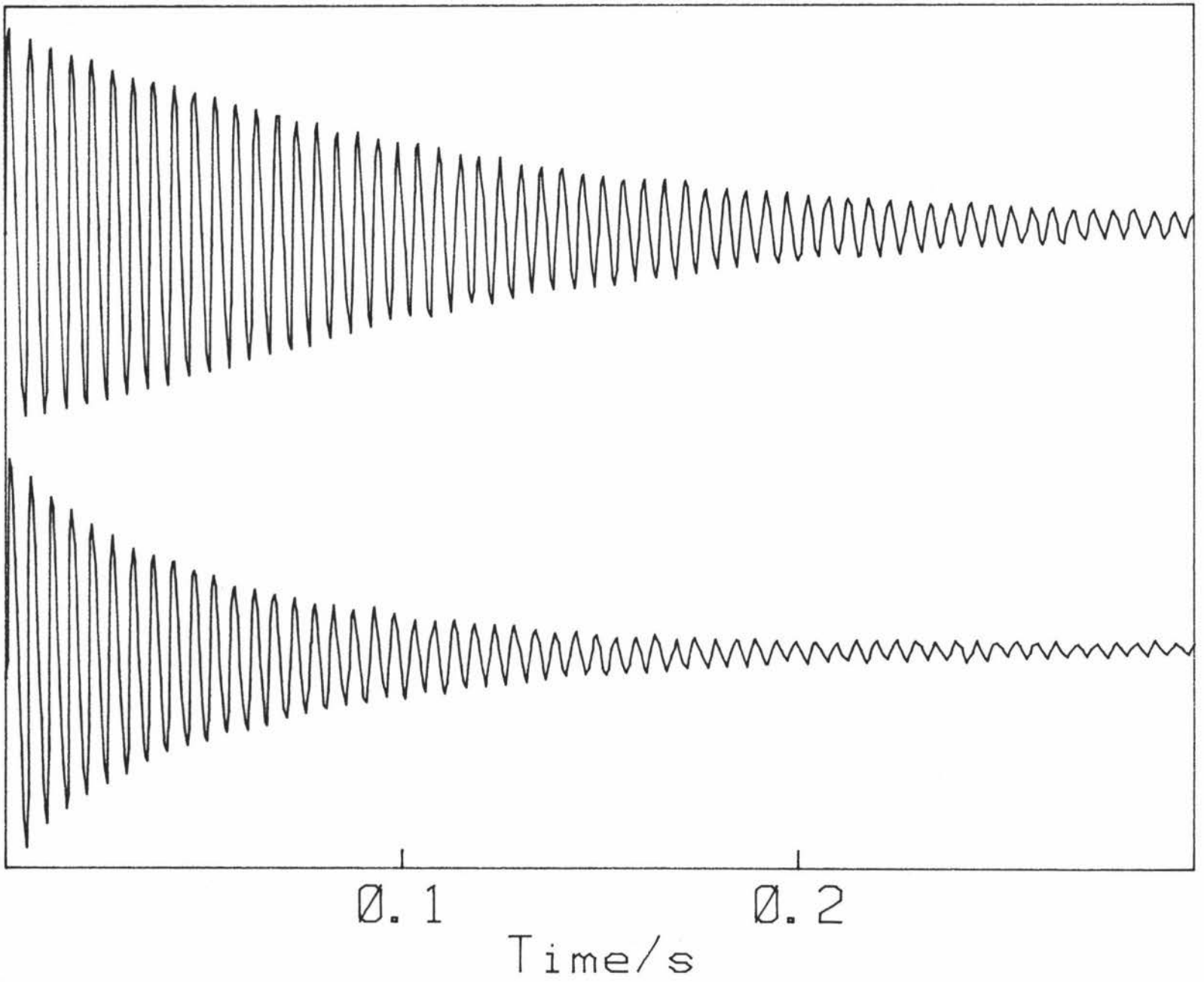
0.1
0.2
Time/s

Figure 11. Deuterium quadrupole splitting of D_2O versus temperature for a 51.30 wt% APFO/D_2O sample illustrating the discontinuity in the temperature dependence of the splitting at T_{NI}

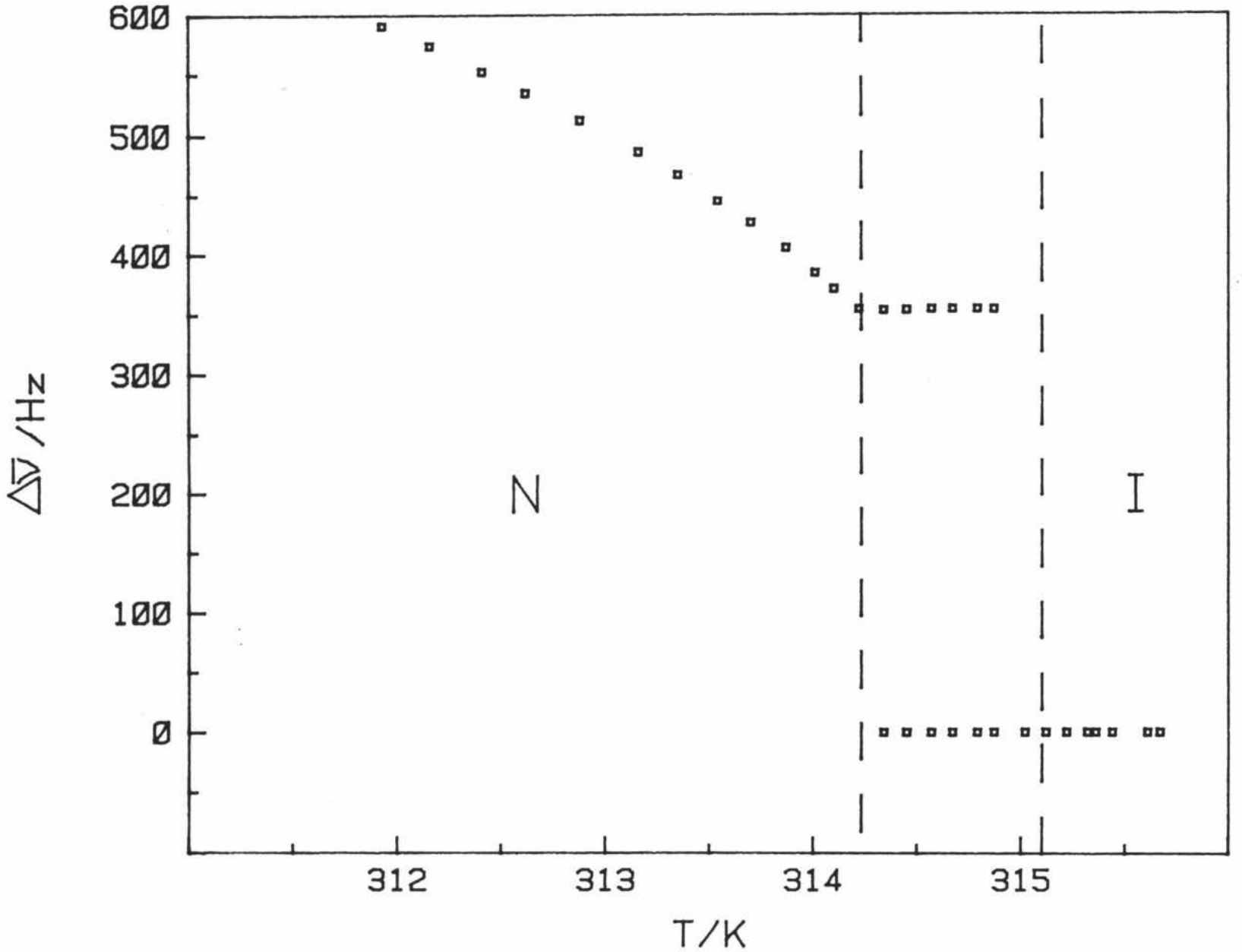
600
500
400
300
200
100
0
Δν /Hz
N
I
312
313
314
315
T/K

small for a separate singlet to be observed and so an averaged doublet spectrum is observed with a quadrupolar splitting of less than that obtained for the slow exchange cooling data. In time as the size of the isotropic domains increases the doublet splitting will increase to the cooling value and the spectrum will sharpen with the eventual appearance of the isotropic singlet. So the first appearance of a singlet on heating from the pure nematic phase as a method for finding T_{NI} is unsatisfactory for the same reason that the observation of the first formation of a nematic doublet on cooling is not a good method for determining T_{IN}. The lack of an observable doublet just below T_{IN} on cooling and the lack of a singlet on heating just above T_{NI} could be interpreted as supercooling and superheating respectively however this phenomenon has been shown to be a kinetic rather than a thermodynamic effect and is associated with domain growth within the colloidal dispersion. Direct evidence for the growth of the colloidal domains has been obtained by cooling a 40 wt% CsPFO/D_2O sample into the middle of the mixed nematic/isotropic phase. After two days a faint boundary line was evident about half way down the sample due to the slightly different refractive indexes of the nematic and isotropic phases. On viewing the sample through cross polarisers a lower liquid crystal phase and an upper isotropic phase could be clearly seen the relative amounts of the two phases being approximately equal, as expected. The two phases, both of which have water as the continuous phase, are cleary totally immiscible. On tipping the sample on its side the more dense nematic phase gradually displaces the lighter isotropic phase. This was the first direct observation of phase separation in these systems which had been previously been thought of as metastable colloidal suspensions. Phase separation occurs because

of the growth of the nematic and isotropic domains and their eventual separation under gravity is due to the slight density difference between the two phases.

The Nematic/Lamellar Transition.

The sequence of spectra observed when a sample is slowly cooled (100 mK/min) from the nematic phase into the lamellar phase along isopleth B of Fig 8 are shown in Fig 12. Distinct lamellar (outermost) and nematic (innermost) doublets can be distinguished by their responses to rotation of the sample about an axis perpendicular to the magnetic field. The intensity of the lamellar phase spectrum is seen to grow and the nematic to be depleted as the transition is crossed. The first appearance of the lamellar doublet on cooling does not however correspond to the upper temperature boundary (T_{NL}) of the nematic/lamellar mixed phase region (c.f T_{IN}). Initially on cooling to below T_{NL} a broadening of the lamellar doublets is observed and it is necessary to wait for a time which decreases with increasing amphiphile composition for the resolution of the separate nematic and lamellar doublets. As the amphiphile composition increases so does the frequency difference between the nematic and the lamellar doublets ($\delta\tilde{\Delta\nu}$) and for a given domain size the slow exchange condition becomes increasingly probable. The broadening phenomenon followed by eventual resolution of doublets is beautifully illustrated for the 51.30 wt% APFO sample in Fig 13. Once slow exchange conditions are reached the nematic and lamellar doublet splitting change little with temperature ($\bar{P}_2$ increases and $\tilde{q}_{zz}$ decreases) until, on reaching T_{LN} when only lamellar phase is present, the lamellar quadrupole splitting begins to increase again with decreasing temperature ($\bar{P}_2$ increases). Both T_{NL} and T_{LN} are obtained from the intersection of the mixed phase lines

Figure 12. Deuterium NMR spectra of D_2O for a CsPFO/D_2O sample obtained on cooling along isopleth B of Fig 8.

(a) Pure nematic.

(b) Just into the mixed phase region.

(c) In the centre of the mixed phase region.

(d) Close to T_{LN}

(e) Pure lamellar.

From Ref. 15.

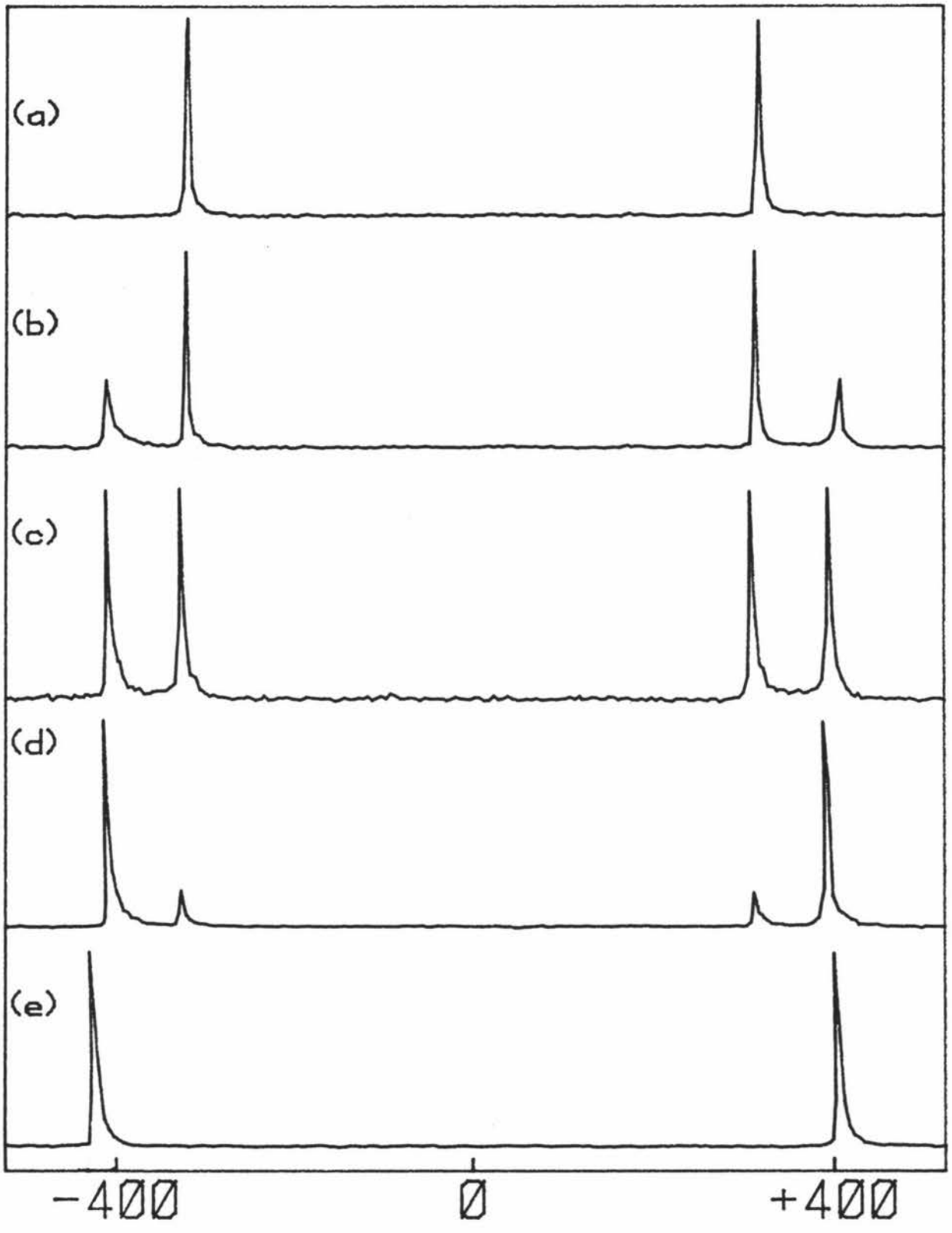
(a)
(b)
(c)
(d)
(e)
−400
0
+400
Frequency/Hz

Figure 13. Deuterium NMR spectra of D_2O for the 51.3 wt% APFO sample as it is cooled from the pure nematic phase into the nematic/lamellar mixed phase.

(a) Pure nematic.

(b) Mixed nematic/lamellar phase with the doublets showing considerable broadening.

(c) 30 minutes after (b) and the start of resolution of separate doublets.

(d) 20 minutes after (c) and good resolution of separate doublets.

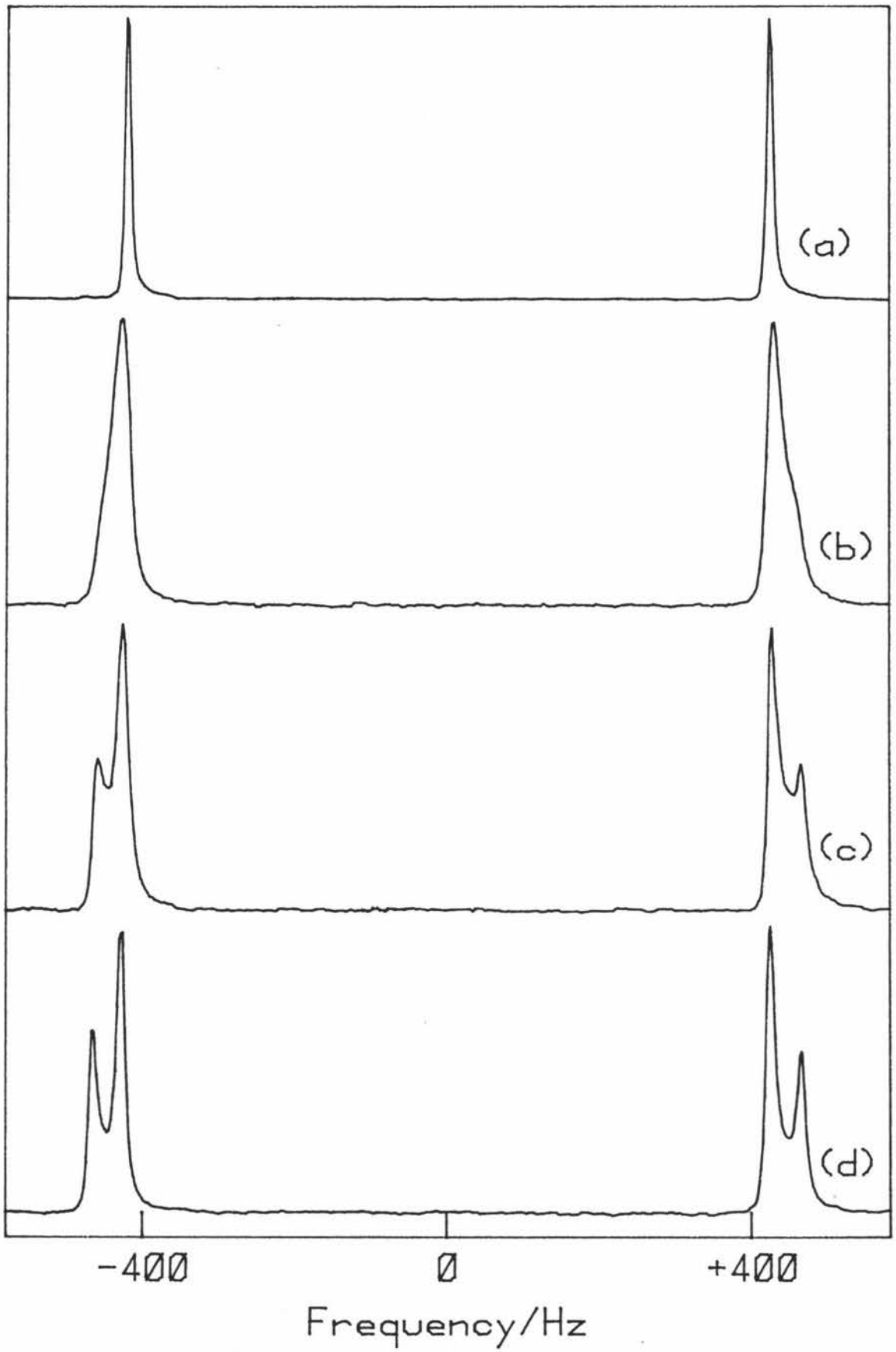
(a)
(b)
(c)
(d)
-400
0
+400
Frequency/Hz

with the pure phase curves. Again it is important to point out that if T_{NL} and T_{LN} are to be determined by the appearance of a lamellar doublet on cooling and a nematic doublet on heating erroneous results will be obtained because of the kinetic effects fully discussed in the previous section.

As the amphiphile composition decreases so does $\delta\Delta\tilde{\nu}$ and separate signals from the two phases become harder to resolve. A limit to the resolution of the two phases is reached at 51.3 wt% for the APFO sample and 53.5 wt% for the CsPFO/D_2O sample. Initially, for both these samples, separate doublets are not observed but rather a broadening of the doublet components which reaches a maximum before eventually sharpening again as the temperature continues to be lowered into the lamellar phase. On waiting thirty minutes at the temperature of maximum broadening separate doublets of equal intensity are eventually resolved and adjustment of the temperature is accompanied by a change in the relative intensities of the doublets as expected. It is therefore possible to identify T_{LN} and T_{NL} from the intersection of the mixed phase and pure phase $\Delta\tilde{\nu}$ lines as for the more concentrated samples. It is also possible to identify T_{NL} with the discontinuity in the temperature dependence of $\Delta\tilde{\nu}$ which is observed on cooling under fast exchange conditions,(Fig 14). The behaviour of the $\Delta\tilde{\nu}/T$ plot for compositions less than Tcp is shown in Figure 15. No mixed phase region is detected from the resolution of separate nematic and lamellar doublets. As the boundary is approached the line exhibits increasing curvature, as in the case for the 51.3 wt% and higher amphiphile composition samples, but no discontinuity in the quadrupole splitting is observed. There is however a discontinuity in the temperature

Figure 14. Partially averaged quadrupole splitting of D_2O as observed on cooling through the nematic to lamellar transition in a 53.9 wt% CsPFO/D_2O sample. The open squares in the mixed phase region were obtained under fast exchange conditions a short time after cooling into this region. On waiting for about 30 minutes the broad peaks resolved into two pairs of doublets (see also Fig 13) corresponding to nematic and lamellar phases, the splittings for which are indicated by the filled squares. T_{NL} and T_{LN} are identified with the intersection of the pure phase curves with those of the mixed phase region as shown. It is also clear that in the fast exchange regime T_{NL} is indicated by the discontinuity in the temperature dependence of the quadrupole splitting.

From Ref 15.

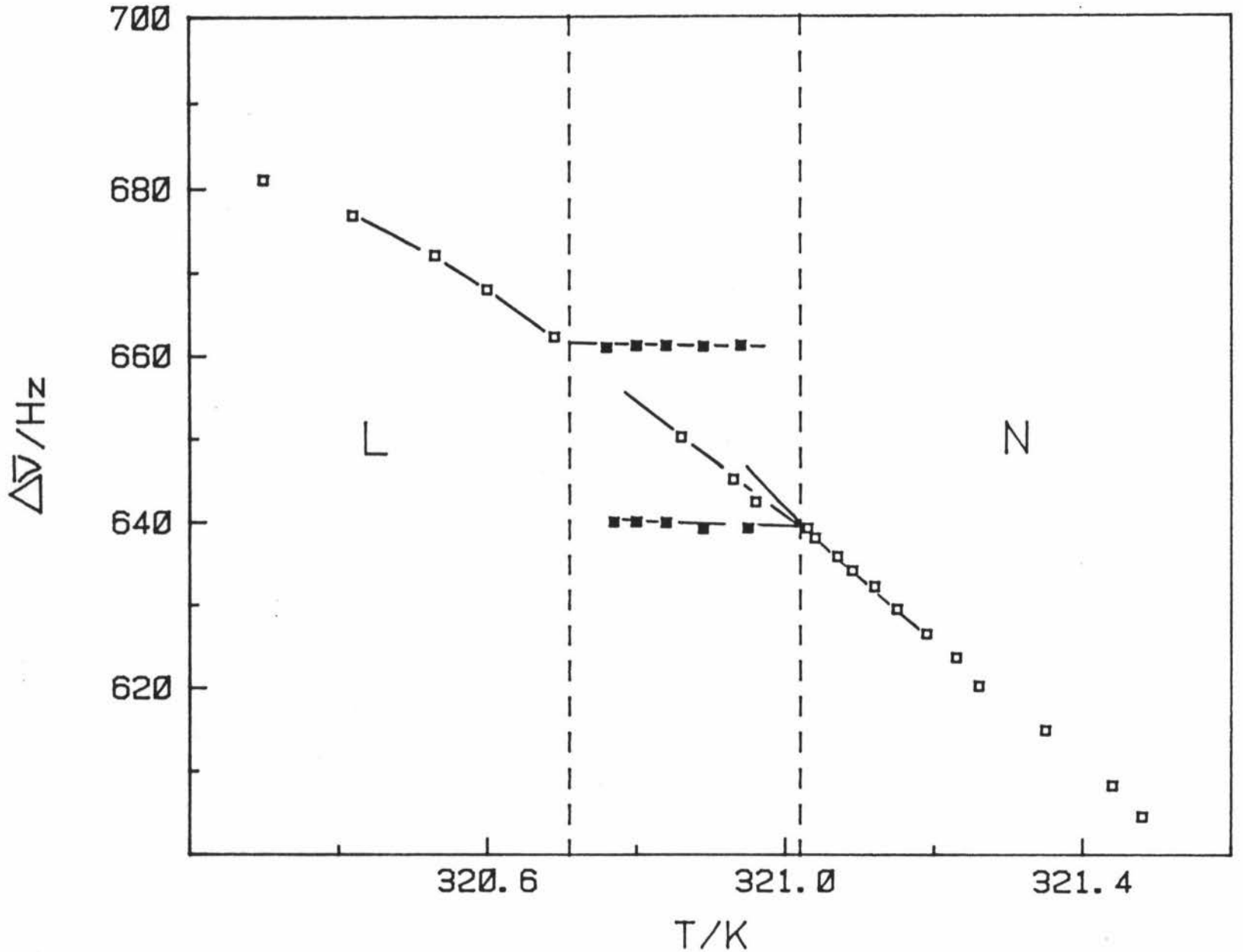
700
680
660
640
620
Δν/Hz
L
N
320.6
321.0
321.4
T/K

Figure 15. Deuterium quadrupole splitting of D_2O versus temperature for a 49.50 wt% APFO/D_2O sample as it is cooled from the nematic phase to the lamellar phase. The dotted line corresponds to T_{NL} and is the break point in the temperature dependence of the quadrupole splitting. T_{NL} may or may not also be equal to T_{LN}

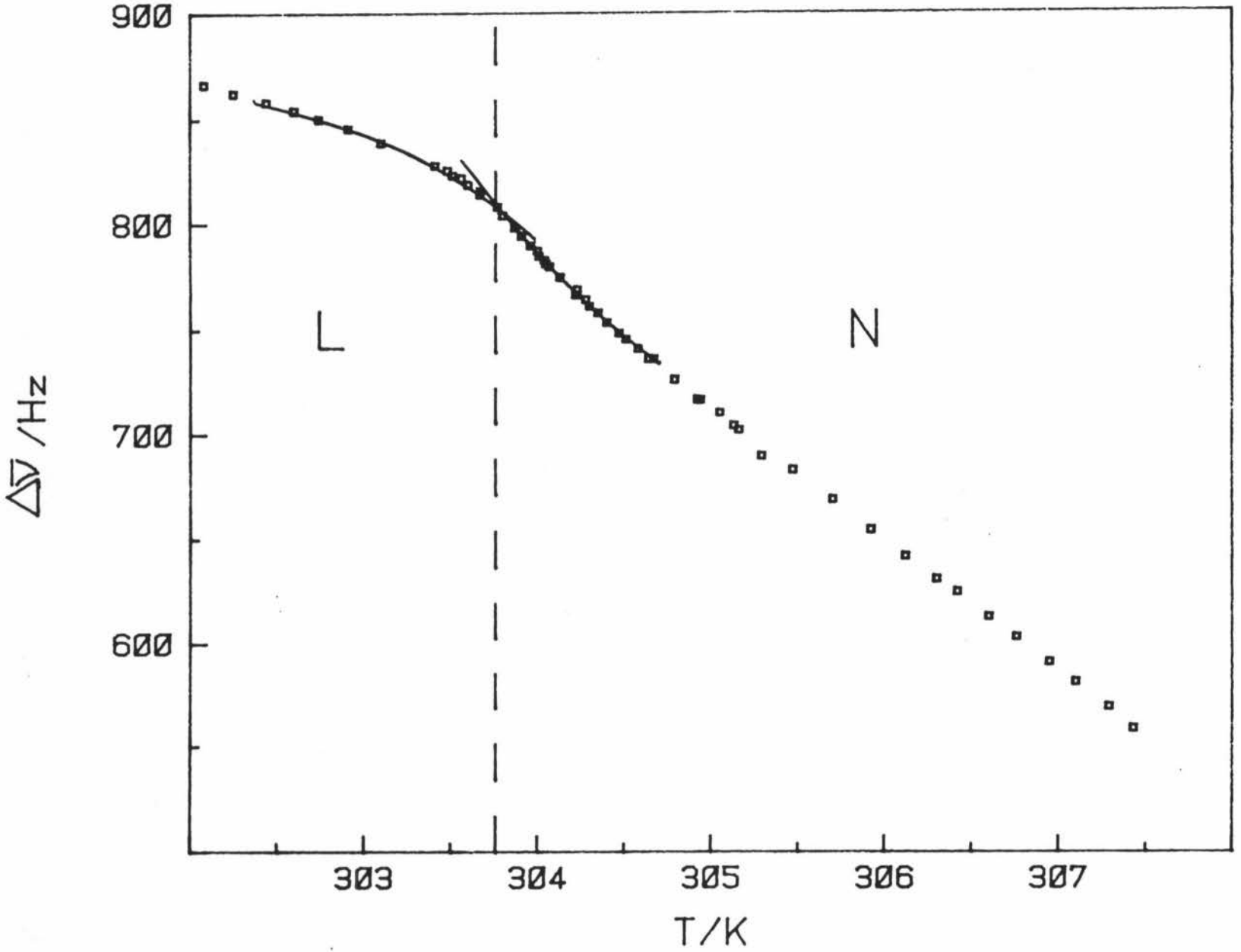
900
800
700
600
Δν /Hz
L
N
303
304
305
306
307
T/K

dependence of the quadrupole splitting which may be identified with T_{NL} (see Fig 14). By using small temperature increments this temperature may be determined very accurately as may be seen from Figure 15. The question that must be answered is whether this temperature also represents T_{LN} (i.e the nematic to lamellar is of second or higher order) or whether the mixed phase region is so narrow that deuterium NMR is unable to detect it. To illustrate this point consider the 51.3 wt% APFO sample. The intermediate exchange condition which is experience in this sample requires $\tau \approx 1/(\pi \delta\tilde{\Delta\nu})$. The value of $\delta\tilde{\Delta\nu}$ is 20Hz which gives a value of 1.6×10^{-2}s. The r.m.s displacement of a water molecule during this time is 5700 nm which may be compared with 740 nm minimum domain size for the isotropic/nematic transition. So in order to observe separate nematic and lamellar doublets the domains must grow to the order of 6000 nm. The temperature and composition intervals of the mixed nematic/lamellar phase region of the 51.3 wt% APFO sample are 0.35 K and 0.3 wt% respectively. Taking into account that the composition and temperature width of the mixed nematic/lamellar phase continues to decrease with decreasing amphiphile composition so that $\delta\tilde{\Delta\nu}$ will become even smaller, it is clear that the domain size will need to be even bigger in order for the doublets to be seen. Thus the detection of separate nematic and lamellar doublets becomes increasingly improbable and may be even impossible as the composition and densities of the two phases converge. So it is not unreasonable to continue to assume a weak first order mechanism for the nematic to lamellar phase transition at amphiphile compositions which are less than Tcp rather than a change over to a second order mechanism at this point. Tcp may well be an artifact of the NMR measurements. Experiments are now being undertaken to resolve this problem and in the

meantime it is better to refer to Tcp as an apparent tricritical point.

The Isotropic/Lamellar Transition

When cooling a sample from the isotropic phase into the isotropic/lamellar mixed phase region the lamellar doublet does not appear until, in some cases, at least 0.5 K below T_{IL}. The main reason for this is that the small lamellar domains are much slower to orientate in the magnetic field which leads to broad, poorly defined doublets which are difficult to detect. In addition the large difference in composition and the consequently large difference between the phases causes phase separation if the sample is left for the long time required for resolution of the lamellar doublets. For these reasons it is best to determine T_{IL} by the same method as that used to determine T_{IN} i.e. from the reduction in the time constant of the FID as was illustrated in Fig 10. The effect is even more marked than is the case for T_{IN} determinations because of the large quadrupole splitting of the lamellar doublets at high amphiphile compositions.

T_{LI}

The determination of T_{LI} is not easy because of problems with phase seperation. In the high concentration regime the difference in compositions of the two phases is large. The resulting large difference in density between the two phases results in the more dense lamellar phase domains gravitating towards the bottom of the sample tube. This means that slow cooling through the mixed phase region will give rise to a false result for T_{LI} because the portion of the sample that lies within the sampling coils will be more rich in amphiphile than its nominal composition. To avoid this problem rapid cooling must be employed although this gives bad orientation within the sample and therefore very broad peaks . The least unsatisfactory method of

determination of T_{LI} is to rapidly cool the sample whilst occasionally removing it from the spectrometer to keep it agitated and to look for the disappearance of the isotropic singlet. If the sample is heated from the homogeneous lamellar phase the isotropic singlet will not appear at T_{LI} because the small size of the isotropic domains that initially form will prevent the observation of a separate isotropic signal. The NMR technique gives good precision for T_{IL} but it gives poor precision for T_{LI}.

Determination of the Triple Point Tp(I,N,L)

The triple point temperature can be found by cooling a sample of composition just above that of the triple point. The samples chosen were 59.6 and 64 wt% amphiphile for the APFO/D_2O and CsPFO/D_2O systems respectively. When a sample is cooled along isopleth C of Fig 8 a sharp decrease in the FID time constant occurs at T_{IL} (point a) which then increases on cooling as the domain size increases and slow exchange takes over. The time constant of the FID rapidly decreases again when the triple point temperature is reached (point b) and nematic phase is formed. On cooling to below Tp(I,N,L) (point c) and in time, a nematic doublet is observed which grows at the expense of the isotropic singlet until only the nematic and lamellar doublets remain. The value for Tp(I,N,L) is too low if it is taken as the first appearance of the nematic doublet for the same reasons as were given in previous sections,i.e the domains are initially too small to give a separate nematic signal. On heating the sample the nematic phase doublet disappears and the singlet reappears as expected, but these observations are not reversible. On cooling the sample once again the nematic phase did not appear at all and only the isotropic and lamellar

signals were seen. The reason for this was evident when the sample was removed and viewed through cross polarisers. The sample was divided into two parts with a dark portion characteristic of the isotropic phase on the top and a transluscent portion characteristic of the lamellar phase on the bottom. This increased composition of the lower half has a T_{LI} above Tp(I,N,L) and therefore no nematic phase was produced in the region of the sample coils of the NMR probe. As was the case for isotropic/lamellar transitions phase separation takes place because of the large composition and hence the large density difference between the nematic and lamellar phases (Fig 8).

DSC

The thermograms were always obtained by heating because supercooling below the solubility curve readily occurs for the APFO/D_2O system. Two peaks are evident in the thermograms of the amphiphile solutions if the sample is first completely frozen to below into the HI/C region (Fig 16). The peak corresponding to the low temperature transition is the larger of the two and occurs at a temperature which is independent of amphiphile composition. The onset of this peak coresponds to the melting of heavy ice at the temperature Tp(HI,I,C). The second of the two peaks is broader and corresponds to the gradual solubilisation of the crystalline amphiphile. The solubilisation peak is small in comparison to the the heavy ice melting peak and therefore its resolution is poor. Better resolution can be obtained by supercooling the sample to just below the Tp(HI,I,C) and waiting for the crystal to drop out of solution. The precipitation of the amphiphile crystals from solution can be monitored by looking for the latent heat of solubilisation detected on the thermal analysis data station. A DSC trace for a sample prepared in this manner shows the solubilisation

Figure 16. The DSC thermogram for a 49.5 wt% APFO/D_2O sample which has been cooled into the HI+C phase prior to heating.

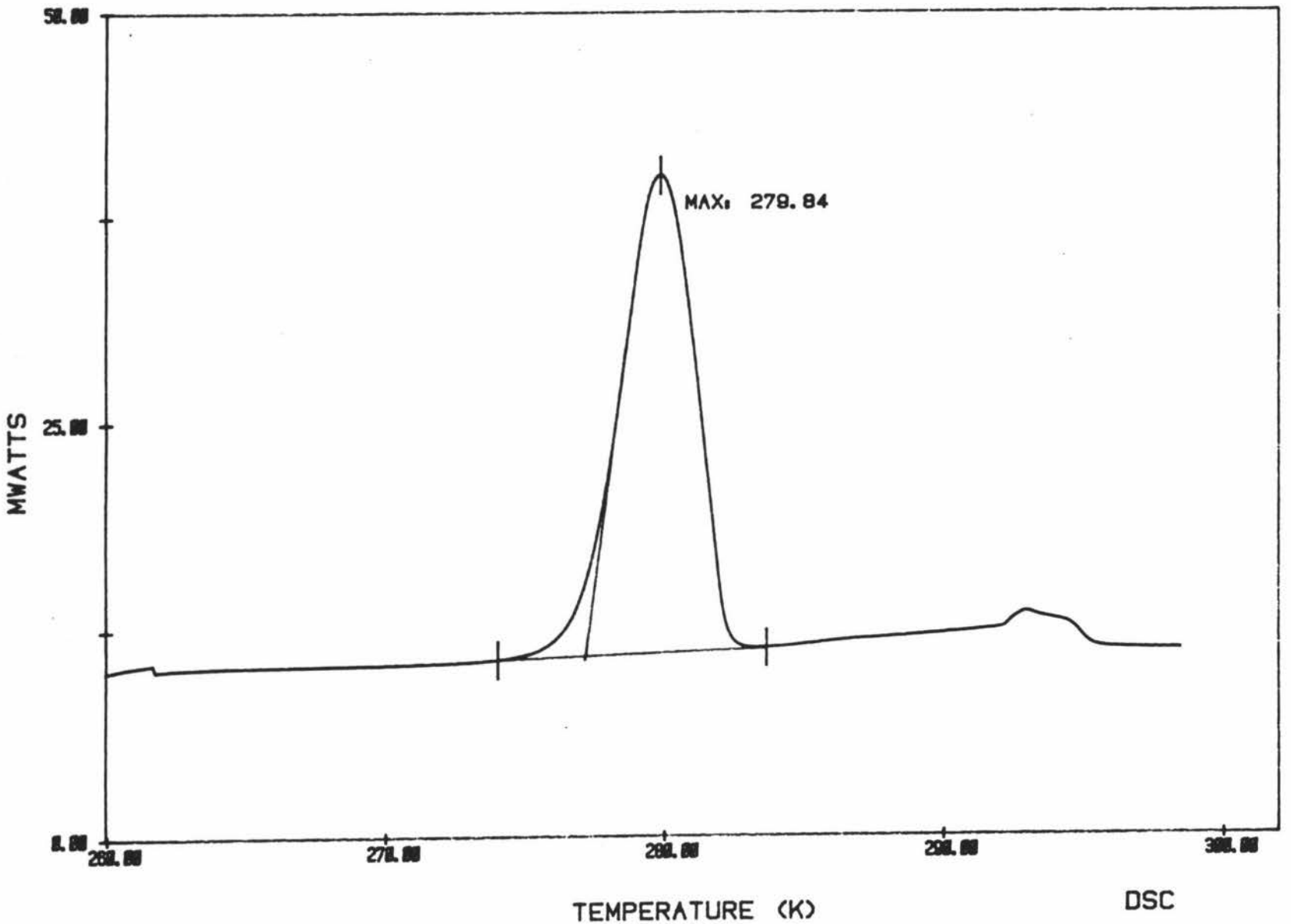
MAX: 279.84
MWATTS
TEMPERATURE (K)
DSC

peak more clearly. The solubilisation peak is not a sharp peak and the reason for this can be seen by looking at the solubility curve Tc. The shape of the I+C region on the phase diagram shows that initially for a sample being heated , the solubility increases very slowly until it reaches the `elbow' of the solubilty curve where a dramatic increase in solubilty occurs. This sudden increase corresponds to the sharp change in peak shape and the peak maximum to the corresponding point on the Tc curve. The shape of the solubilisation curve obtained varied with composition. For more dilute samples e.g. 21.3 wt% (Fig 17) the peak was small with only a small gradual increase before the peak proper began. As the amphiphile composition was increased to 49.5 wt% (Fig 18) a second peak became apparent. This peak corresponds to the transition from L+C to L and the low temperature peak to the transition I+C to L+C. In the 59.7 wt% sample (Fig 19) the second peak dominates the shape of the thermogram. This implies that the temperature range of the L+C region is on the increase compared with the constant range of the I+C region at compositions greater than Kp.

The liquid crystalline phase transitions can be detected by using the DSC technique but it is not possible to obtain precise information on the transition temperatures. The liquid crystal phase transitions involve very low energy changes and this means the peak are of very low intensity.

DSC has proved to be a very useful technique for defining the solubility curve and some of the other transitions of the system being studied. Although NMR can be used for some of the transitions involving solid to liquid crystal, the DSC method is faster. The DSC

Figure 17. The DSC thermogram for a 21.3 wt% APFO/D_2O sample. This sample was prepared by cooling until the amphiphile crystals were deposited from solution but the D_2O existed as as supercooled liquid.

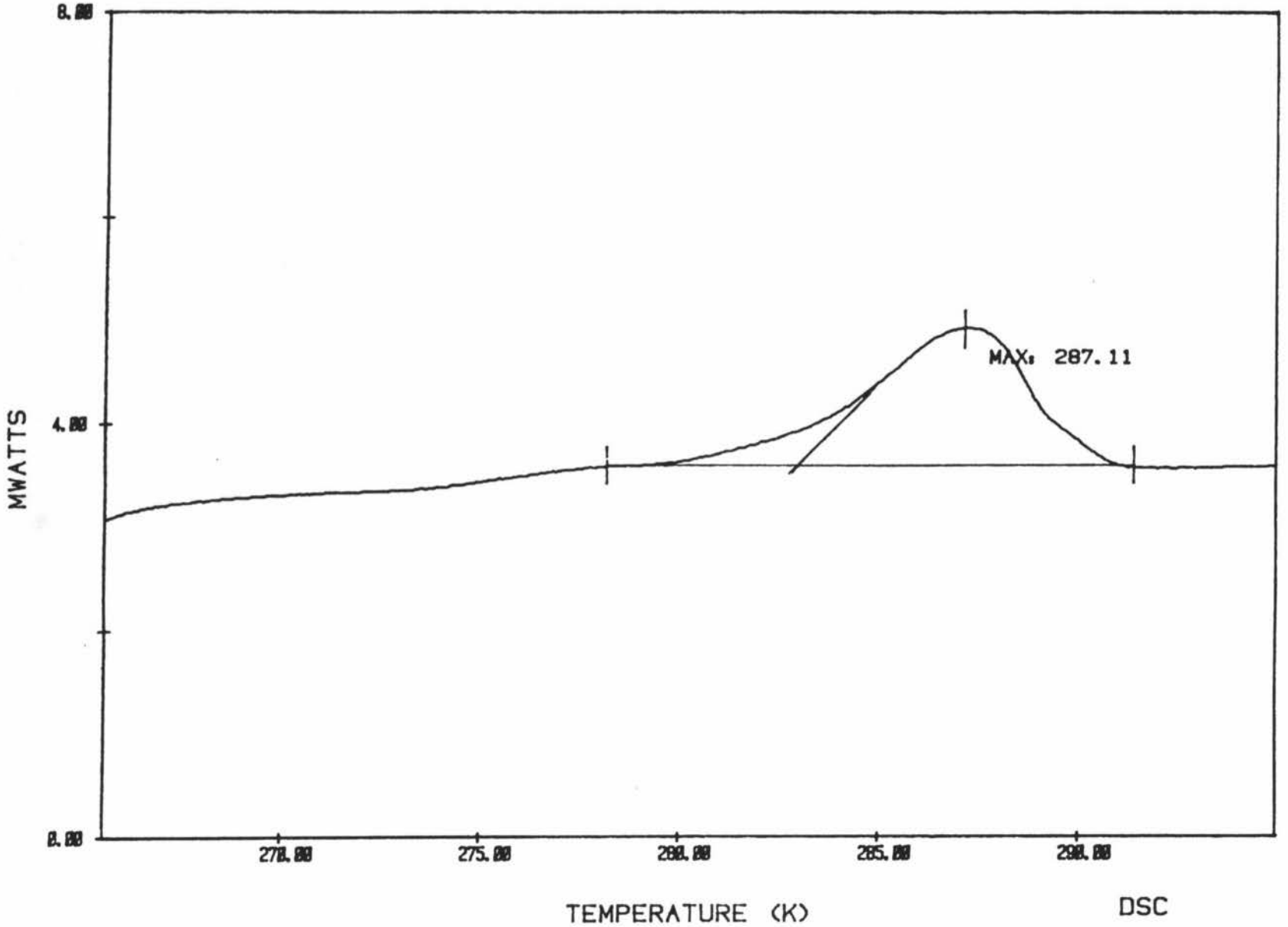
8.00
4.00
0.00
MWATTS
MAX: 287.11
270.00
275.00
280.00
285.00
290.00
TEMPERATURE (K)
DSC

Figure 18. The DSC thermogram for a 49.5 wt% APFO/D_2O sample. This sample was prepared by cooling until the amphiphile crystals were deposited from solution but the D_2O existed as as supercooled liquid.

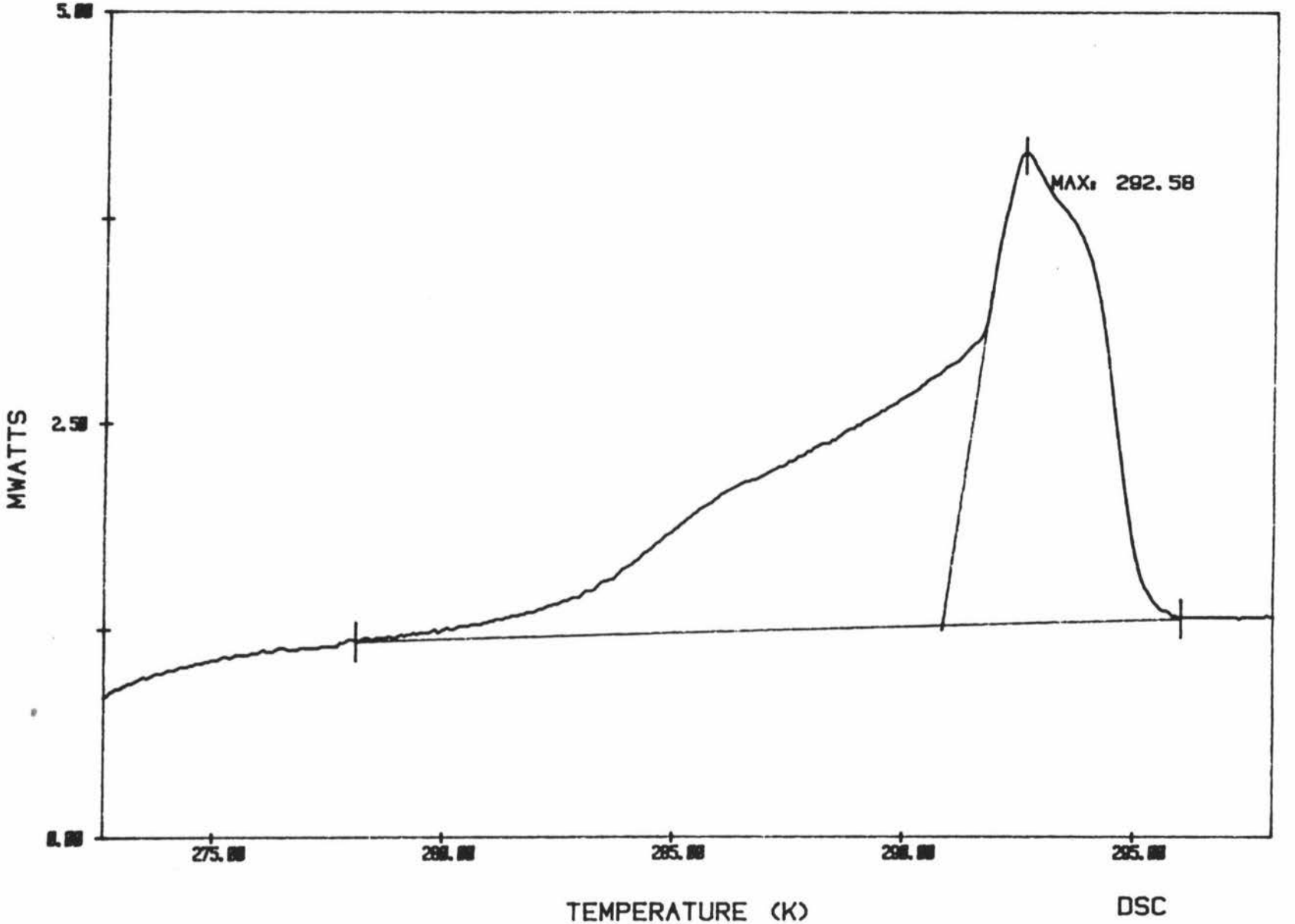
MAX: 282.58
MWATTS
TEMPERATURE (K)
DSC

Figure 19. The DSC thermogram for a 59.7 wt% APFO/D_2O sample. This sample was prepared by cooling until the amphiphile crystals were deposited from solution but the D_2O existed as as supercooled liquid.

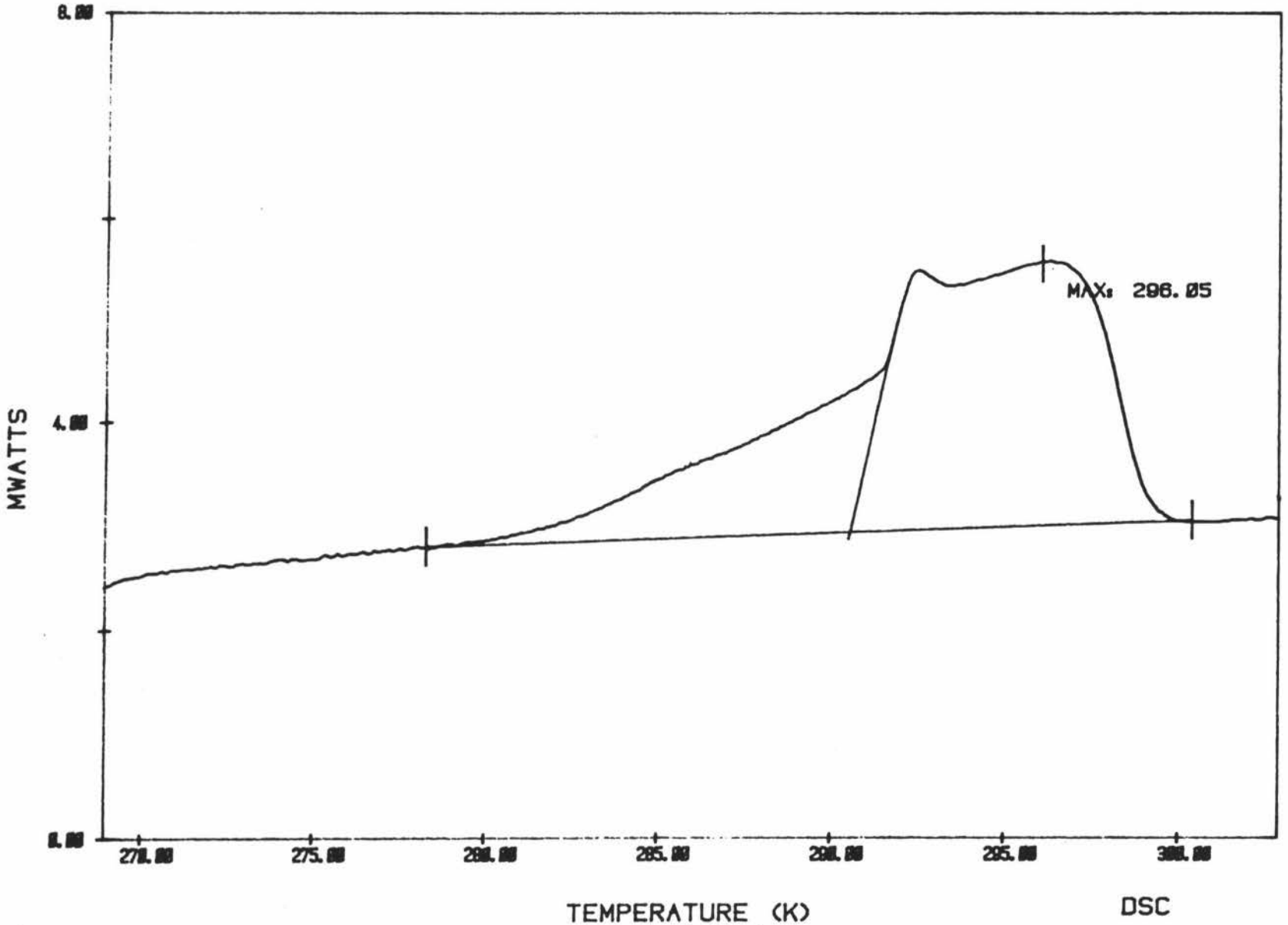
MAX: 296.05
MWATTS
TEMPERATURE (K)
DSC

is limited in its usefulness however because it cannot give the transition temperatures to any great precision.

Conductivity

Determination of the Solubilty Curve

The solubility curve in the region of 0 to 15 wt% amphiphile was determined from conductivity measurements. These measurements were used in conjunction with the DSC results to define the solubilty curve across the complete range of amphiphile compositions up to 60 wt%. The method used to determine the solubility of each of the samples was to supercool the sample until crystallisation took place and then to reheat until the conductivity on heating matched the conductivity on cooling. The cooling curve initially shows a linear dependence on temperature. This continues past Tc , because of supercooling , until crystallisation begins to occur. When crystalisation occurs there is a sudden drop in conductivity as the amphiphile comes out of solution which gradually slows until it reaches the initial rate of change of conductivity with temperature. This sigmoid curve is also seen on heating the sample. On heating the conductivity increases slowly in the beginning and then rapidly as the bulk of the solubilisation takes place and then slowly again until the heating curve merges with the cooling curve at Tc (Fig 20). The resultant solubility curve increases sharply with temperature up to 286.5 K and from there on shows only a slight increase over the rest of the composition range. The significance of this shape is that the amount of amphiphile dissolved in the solution increases only slightly as the temperature increases up to 286.5 K and from then on increases rapidly with small temperature increments. Heating from 282 K to 286.5 K (a 4.5 K range) increases the weight percentage of amphiphile from 2 to 7 whereas heating from

Figure 20. The temperature dependence of the electrical conductivity of a 7.48 wt% APFO/D_2O sample on cooling (+) and on heating (□). The intersection of the curves gives Tc.

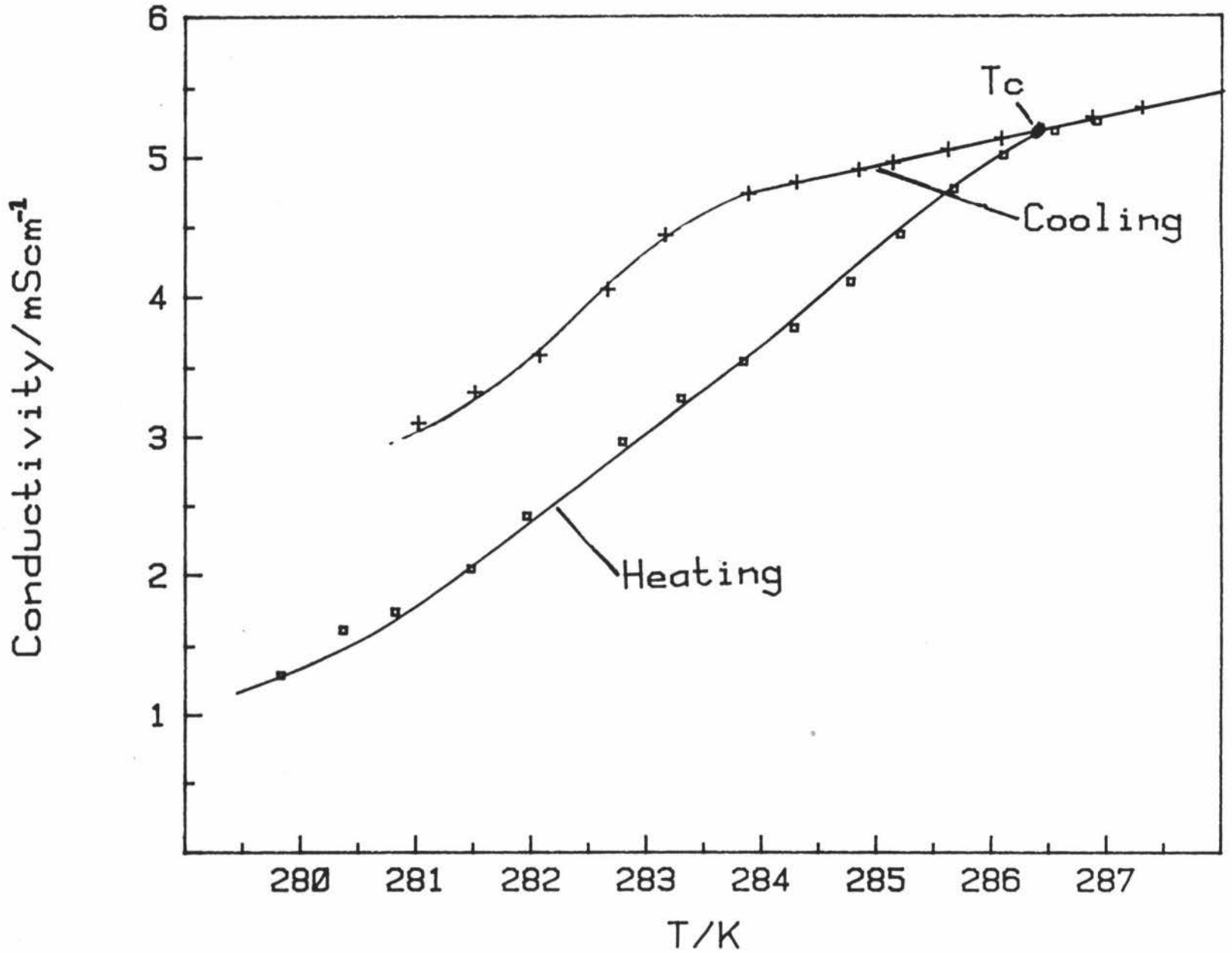
Conductivity/mScm-1
6
5
4
3
2
1
Tc
Cooling
Heating
280
281
282
283
284
285
286
287
T/K

286.5 K to 290 K (a 3.5 K range) increases the weight percentage of amphiphile from 7 to 40. This rapid increase in solubility occurs at a temperature greater than that of the Krafft point which is expected since the onset of micellation dramatically increases the solubilty of amphiphiles in water.

Determination of the Critical Micelle Concentration

The conductivity has a different dependence on temperature above the c.m.c than it has below it. Use of this property can be made to locate the c.m.c by taking the intersection of these two sets of data. The c.m.c was therefore defined as the discontinuity in the rate of change of conductivity with concentration (Fig 21). The c.m.c was determined at three different temperatures ; 25 , 45 and 65^{o}C.

The c.m.c composition at the three temperatures studied are within 5% of each other indicating a ΔH at micellation of ≈ 0. This result agrees with recent work done on the NaPFO/H_2O system [19]. The value of the c.m.c for the APFO/D_2O system was determined to be 1.1 wt% amphiphile or 2.5×10^{-2} mol kg^{-1} and the Krafft point was at 279.2 K.

Figure 21. The dependence of the electrical conductivity of APFO/D_2O samples on amphiphile composition at three temperatures. The break points in these plots corresponds to the c.m.c.

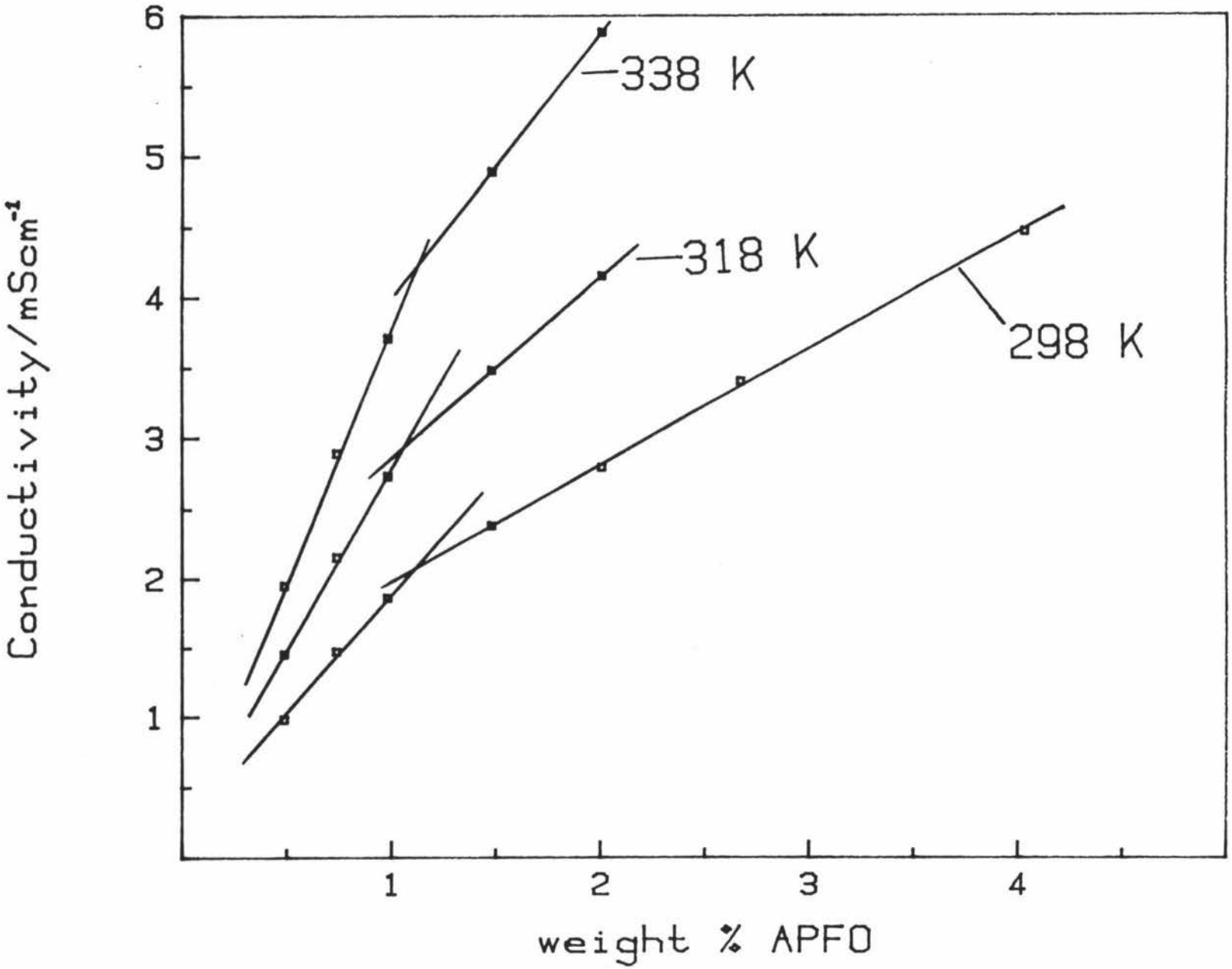
Conductivity/mScm⁻¹
6
5
4
3
2
1
338 K
318 K
298 K
1
2
3
4
weight % APFO

Discussion

The first qualitatively and quantitatively accurate phase diagram to be reported for an amphiphile/water system was the CsPFO/D_2O system [14] as shown in Figure 1. The phases were identified by microscopy, NMR and X-ray diffraction [15] and precise and accurate phase transition temperatures were determined by careful temperature control of the sample. The system is an attractive one for experimental studies of mesophase structure, properties and phase transformations since it is a binary system with an extensive N_D^+ phase and macroscopic samples of both nematic and lamellar phases with homeotropic director distributions can easily be obtained by simply cooling from the isotropic phase in a magnetic field. The second qualitatively and quantitatively accurate phase diagram to be completed is the APFO/D_2O system reported in this thesis and shown in Figure 5. As was stated in the introduction one of the aims of this study was to obtain such a phase diagram and this has been accomplished over the full concentration range of the nematic phase. The second aim was to investigate the effect of changing the counter ion on the nature of the mesophase structures and phase transformations. Comparison of these two phase diagrams shows them to have the same general form and they show similar responses to NMR, DSC and conductivity measurements. The conclusion is that the structure of the phases which have been established for the CsPFO/D_2O system [11,13,14,20](ie Isotropic micellar:- solution of discoid micelles with random distribution of their symmetry axes; Nematic:- solution of discoid micelles with long range orientational ordering of their symmetry axes and lamellar:- solution of discoid micelles with long range orientational and translational ordering of their symmetry axes) is reflected in the

APFO/D_2O system. Thus, changing the counter-ion in this instance has not effected the nature of the liquid crystalline mesophases present. It is also clear that while the two diagrams are qualitatively identical they differ quantitatively in the thermodynamic state (temperature and composition) of the system necessary to bring about the various phase transition.

In the ensuing discussion, the implications of the phase diagram concerning the nature of the lamellar to nematic and nematic to isotropic transitions will be described. The quantitative differences in the phase diagrams will be interpreted in terms of the factors which control the stability of the micelles and finally the significance of the various triple points will be discussed.

(i) Nematic to isotropic transition and nature of the nematic phase.

The assertion that the nematic phase is a solution of discoid micelles with long range orientational ordering of their symmetry axes has been confirmed by x-ray diffraction measurements for the CsPFO/D_2O system [13,20]. Because of the qualitative similarity between the phase diagrams of the CsPFO and APFO/D_2O systems there is no <u>a priori</u> reason why the nematic phase of the APFO/D_2O system should not also have the same structure. X-ray work to be carried out at Leeds will surely confirm this assumption. The picture that is emerging for the CsPFO/D_2O nematic phase and by implication the APFO/D_2O nematic phase, is that the micelles diameter is roughly of the order of separation of the centres of mass of the micelles over the entire composition range of the nematic phase (between 0.1 and 0.43 volume fraction and 0.25 and

0.51 volume fraction of amphiphile for the CsPFO/D_2O and APFO/D_2O systems respectively). The occurence of such an extensive nematic phase for both the Cs and APFO/D_2O systems is contrary to the fundamental postulate invoked in models to explain the concentration dependence of the structures of aqueous solutions of amphiphilic compounds [21] which is that the dominant inter-aggregate interaction is repulsive (electrical double layer, excluded volume or hydration force) and that the associated contribution to the free energy of the system is minimised by reorganisation of the amphiphilic molecules into a smaller member of larger aggregates which would favour the formation of bilayers (lamellar phases) in concentrated solutions. It has therefore been suggested that the nematic phase is intrinsically unstable [22] and it has been postulated that nematic phases are really defective lamellar phases [12]. X-ray results [13,20,23,24] suggest however that nematic phases exist because, contrary to expectations, small anisotropic micelles are stable over extensive concentration and temperature ranges.

In the Maier-Saupe theory of the nematic phase [25] the potential of mean torque of a cylindrically symmetric particle is given by

$$U(\beta) = -\varepsilon \bar{p}_2 p_2(\cos\beta) \qquad (5)$$

where ε is an interaction parameter related to the nematic to isotropic transition temperature T_{NI} by

$$kT_{NI}/\varepsilon = 0.2202 \qquad (6)$$

It has not been possible to test the applicability of this theory to date because of the absence of a suitable system. The systems discussed here would be ideal for this purpose if meaningful values for $\bar{p}_2$ for the micelles could be obtained. Although work is proceding in

an attempt to determine this parameter and provisional results are availiable [13,20] the measurements to date are not of sufficient accuracy to test the theory directly. Another way of testing equation (6) would be to obtain values for ε. For micelles dispersed in an aqueous medium the variations of with temperature and concentration is expected to be of the form.

$$\varepsilon = \varepsilon_{mm}\Phi_m/V_m = \varepsilon_{mm}c_m \qquad (7)$$

where ε_{mm} is the strength of the anisotropic interaction of the micelles, Φ_m is the volume fraction of micelles which is taken to be the same as the volume fraction of the amphiphile, Φ_A, V_m is the volume of the micelle and c_m is the number of micelles per unit volume. ε_m will vary with the anisotropy of the micelle (the ratio of the major to minor axes of the discoid micelle) which varies with the temperature and composition. The dependence of the micelle anisotropy on temperature and composition has to date been determined only for a 55 wt % CsPFO/D_2O sample from a combination of conductivity and X-ray measurements [13,20] and further work is underway to extend the composition range but the observation that T_{NI} is roughly proportional to Φ_A suggests that equation (6) is at least qualitatively correct.

For both the CsPFO/D_2O and APFO/D_2O systems the quantity $T_{IN}-T_{NI}$ decreases with decreasing amphiphile composition. From 1.36 K at 61.2 wt % amphiphile to 0.10 K at 20.0 wt% amphiphile for the CsPFO system and from 3.15 K at 59 wt% amphiphile to 0.27 K at 35 wt % amphiphile for the APFO system. This quantity is related to the quantity $T_k-T_C^*$, where T_k is the upper bound of the nematic-isotropic coexistence region and T_C^* is the temperature below which the isotropic phase becomes unstable. This quantity has recently been determined

using magnetic birefringence measurements [26,27] and it is found that $T_k - T_C^*$ decreases from 600 mK for a sample with 56 wt % CsPFO to 20 mK for a sample with 36 wt % CsPFO, a finding which is in line with the NMR results. To explain the observed decrease in $T_k - T_C^*$ it was suggested that the system is crossing over from uniaxial to biaxial behaviour at a Landau point. The phase diagrams give no indication that this is occurring however and the response of the systems to the NMR experiment for isotropic-nematic transitions remains identical throughout the full concentration range of the nematic phase as well as for the supercooled mesophase at compositions less than Tp(I,N,C).

(ii) Lamellar to nematic transition and nature of the lamellar phase.
In both the systems discussed here there are a number of reasons for believing that the lamellar phase consists of planes of discoid micelles and that at the nematic to lamellar transition the nematogenic discoid micelles simply condense on to the planes of the lamellar phase rather than aggregate to form infinitely extending bimolecular lamellae. Firstly there is the NMR evidence of the dependence of the quadrupole splitting of D_2O on temperature across the transition. There is no discontinuous change in $\tilde{\Delta\nu}$ which would result from a discontinuous change in the structure of the aggregates. The small changes observed are interpreted in terms of small changes in $\bar{P}_2$ and $\tilde{q}_{zz}$ (equations 1 and 3) on crossing from the nematic into the lamellar phase. Secondly for a large concentration range the thermodynamic nature of the transition is either weakly first order or second order in which case nematic and lamellar phases differ only with respect to the symmetry properties of the discoid micelles. Thirdly, the electrical conductivity of CsPFO/D_2O samples varies in an analagous

manner to the deuterium quadrupole splitting across the lamellar to nematic transition [11]. While it is recognised that both these qualities are second rank tensor properties, specifically, the conductivity monitors the diffusion of the Cs^+ ions through the mesophase and is, therefore, a structural probe. There is no indication of any large change in the aggregate structure at the transition point rather a small growth of the micelles (0.5%) is indicated. Fourthly, there is no a priori reason why if in the nematic phase finite discoid micelles are thermodynamically stable with respect to infinite bilayer, they should not continue to be so in the lamellar phase. All the above reason strongly support the model of the lamellar phase as planes of discoid micelles having translational and rotational ordering of their symmetry axes. The alternate model for the lamellar to nematic transition considers the transition to be the result of disruptions in the bilayer lamellae by defects such as pores and irregular breaks caused by the aggregation of these pores [12] and whilst this model is not inconsistent with the experimental observations, the concept of a nematic phase consisting of irregular shaped micelles is not very appealing from a chemical point of view.

The temperature of the lamellar to nematic transition for both systems is proportional to the volume fraction of amphiphile as was the case for T_{NI}. The ratio of the two transition temperatures T_{LN}/T_{NI} for both systems remains reasonably constant at 0.98 over the full concentration range of the nematic phase. Since T_{LN} increases with Φ_A this means that the strength of the interaction responsible for this transition must also increase with Φ_A. This simple observation together with the proposed structure of the nematic and lamellar phases enables the

nature of the interaction which causes the transition to be understood. If the attractive interaction was dominant the mutual interaction between micelles would cause them to stick one atop the other to form columns which with decreasing temperature would assemble into columnar phases (hexagonal/tetragonal), behaviour which is in fact observed for thermotropic discoid mesogen molecules where the nematic to columnar phase transition is driven by the mutual attraction of the central aromatic cores. Clearly then the attractive interaction is not dominant in systems of discoid micelles which are precursers of N_D^+ and lamellar mesophases. The long range repulsive interaction (electrostatic double layer repulsion) on the other hand is minimised by arranging the discoid micelles on a cubic lattice. Thus we may envisage a model for the lamellar phase as having the micelles arranged in a face centred cubic lattice with their symmetry axes normal to the (111) planes which would form the lamellar planes. In the most disordered configuration the centres of mass of the micelles will be randomly distributed within the lamellar planes and to a lesser extent in the direction normal to these planes in much the same way as the molecules in a thermotropic smectic A phase. Clearly detail structural investigations are required to establish these models, but it can be concluded on the basis of structural considerations that the interaction driving the translational ordering in the lamellar phase is the long range electrical double layer repulsion between micelles. The strength of this interaction will increase with the volume fraction of the amphiphile and explains the corresponding increase in T_{LN}.

A more quantitative insight into the nature of inter-micelle interactions based on the above model has been obtained by applying the

McMillan theory [28] of the thermotropic smectic A to nematic transition [20]. The liquid crystalline phase behaviour, shown in Figs 1 and 5, was shown to be consistent with a two particle potential containing both isotropic and anisotropic attractive and repulsive long range interactions. The range of the repulsive interaction was found to be greater than that of the attractive interaction and both are of the order of 1.0 to 2.0 nm.

Since T_{LN} is proportional to T_{IN} it follows that the anisotropic interaction which is the cause of the orientational order of the micelles in the nematic phase must also be dominated by the electrical double layer repulsion.

(iii) Stability of micelles

Nematic phases exist because, contrary to expectations, small anisotropic micelles are stable in concentrated solution. At the present time little is known concerning the factors which would favour the stability of nematic phases but they must be related to the stability of the micelles and so the issue to be addressed is what are the factors which govern the stability of micelles in aqueous solution? This thesis is concerned with the effect of changing the counter-ion on the liquid crystal phases and phase transitions. It has already been established that the nature of the phases is unaffected by change of counter-ion Cs^+ for NH_4^+ but that the temperature and composition at which phase transitions occur is affected. In the following section the factors governing the stability of the micelles will be investigated. To facilitate this discussion a comparative phase diagram has been constructed in which the composition axis is mol% PFO^-

so that the specific effect of the Cs^+ and NH_4^+ counter-ions can more readily be observed.

The occurence of a nematic phase over such an extensive range of concentration in the two systems is due to the stability of the lamellar phase which does not give rise to the usual hexagonal phase at high water concentrations invariably encountered for simple hydrocarbon ionic amphiphiles. The reason for this must be in the relative strengths of the various molecular interactions involved and their roles in determining the size and shape of amphiphilic aggregates.

The average chemical potential for a molecule of amphiphile in an aggregate containing N molecules can be written as

$$\hat{\mu}_A = \mu_A/N = \hat{\mu}_A^o + (kT/N)\ln x_A/N + (kT/N)\ln \gamma_A \qquad (8)$$

$_A$ is the chemical potential of a molecule in a single N-aggregate in the solution, the second term is the entropy of mixing associated with the distribution of different sized aggregates each present with mole fraction x_A/N, and the third term represents inter-aggregate interactions. At infinite dilution this equation reduces to

$$\hat{\mu}_A = \hat{\mu}_A^o = \gamma a + c/a + g(a) \qquad (9)$$

where γa is the interface energy arising from the chain-water contact, c/a is the Coulombic repulsion between the charged head groups and g(a) is the free energy associated with the packing of the chains in the aggregate which will depend on the surface area per head group a, the elastic properties of the medium and the interfacial curvature at the particular site in the aggregate.

The first term is independent of the counter-ion and favours the

contraction of the aggregate suface (minimum a). This term is bigger for a fluorocarbon than for the corresponding hydrocarbon for a given head group since the interfacial tension between fluorocarbon and water is greater than that between hydrocarbon and water. The decrease in free energy on transferring a $-CF_2-$ group from an aqueous solution to a micelle is greater than that for a $-CH_2-$ group. This explains why the c.m.c for the two systems (0.025mol kg^{-1} and 0.019mol kg^{-1} and for NH_4^+ and Cs^+ respectively) is comparable with that of a hydrocarbon chain which has a much longer chain length (≈3/2 times bigger).

The second term in equation (9) depends upon the distribution of counter-ions in the electrical double layer at the interface. The simplest model [29] envisages two distinct binding sites with different energies. The lower energy sites are associated with counter-ions which are interposed between neighbouring carboxyl groups, whilst the higher energy sites are associated with ions distributed in a diffuse layer above the carboxyl groups. The distribution of the counter ions over the two sites will be determined by the hydration energy of the ion and also by the temperature. Low hydration energy and low temperatures favour the low energy sites. The presence of counter ions in the low energy sites favours a more planar surface since the polar head group are able to approach more closely and thus discoid micelles and lamellar phases are favoured. Inspection of Figure 22 shows that the Cs^+ salt has lamellar and nematic phases existing at higher temperatures that the NH_4^+ salt over the full PFO^- composition range. This implies a greater portion of the Cs^+ ions in the low energy site at any given temperature than is the case for the NH_4^+ ions. This state of affairs is consistent with the hydration enthalpies of Cs^+ and NH_4^+

Figure 22. Portions of the phase diagrams of the CsPFO/D_2O and APFO/D_2O systems showing the isotropic to nematic and nematic to lamellar phase transition lines. The composition scale is expressed as mol % PFO^- for comparison purposes.

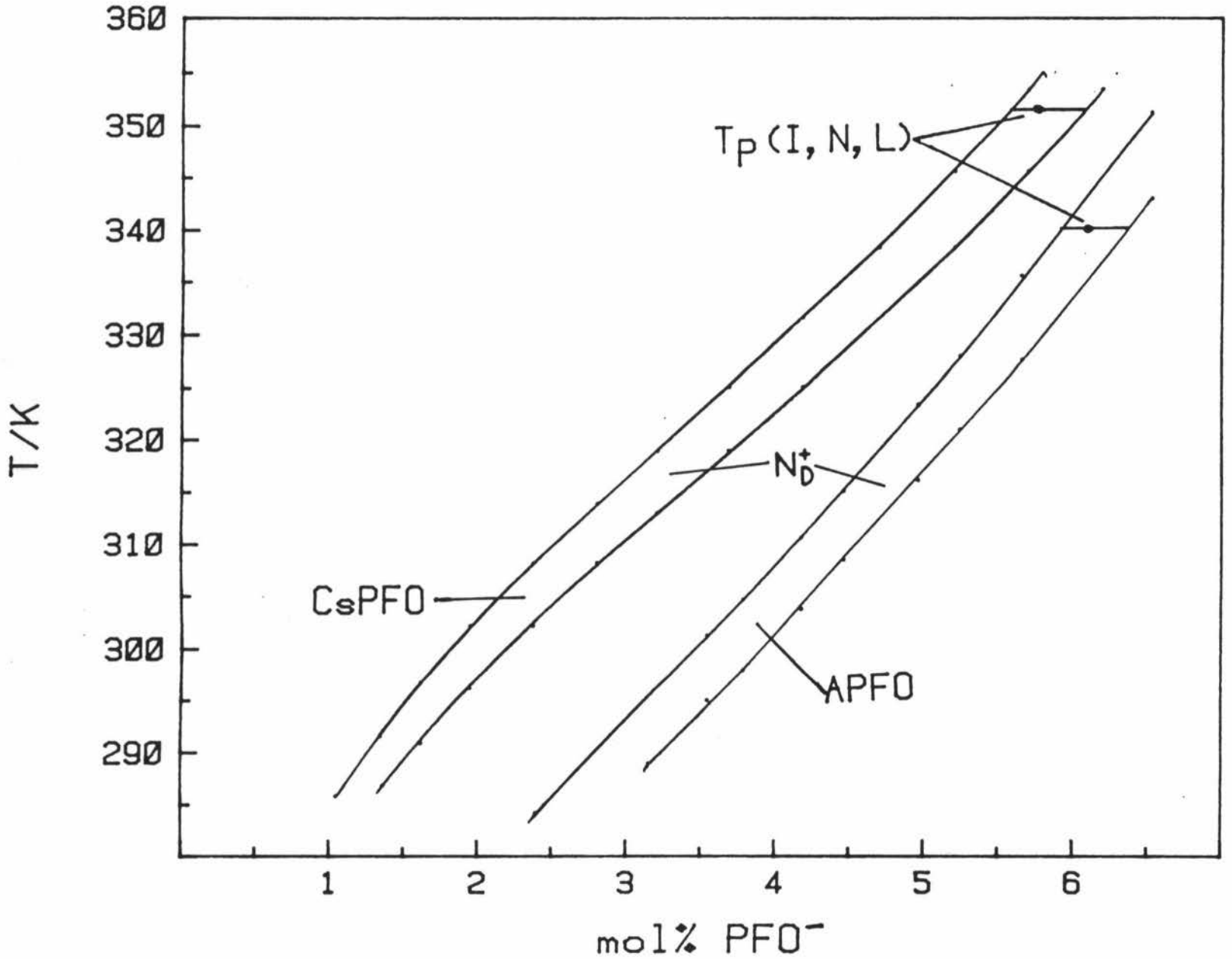
360
350
340
330
320
310
300
290
T/K
T_P (I, N, L)
N_D^+
CsPFO
APFO
1
2
3
4
5
6
mol% PFO^-

ions of -276 and -301 kJ mol^{-1} respectively. Thus the small differences in the two phase diagrams may be interpreted in terms of the small differences in the hydration enthalpies of the two ions.

The third term depends on the chain-chain interaction energy. Little is known about the conformational states of fluorocarbon chains in the liquid state but they are significantly more ordered than their hydrocarbon counterparts and this will make the interior of the aggregate more compressible which in turn favours a planar interface (N_D^+ and L phases). The actual value of g(a) will also depend on the curvature of the interface which in turn is affected by the degree of counter ion binding. It seems probable that as a consequence of interplay between the second and third terms of equation y small oblate elipsoids (discoid micelles) may be energetically favoured with respect to infinite bilayers. For example, there will be a higher probability of the counter-ions residing in the high energy site when in the rim of the disc than in the central core. The proportion of curved to planar interace and, consequently, the diameter of the micelle is expected to decrease with increasing temperature leading to a consequent decrease in the anisotropic interaction which are the driving force for the isotropic to nematic and nematic to lamellar transitions.

In concentrated solutions the third term of equation 6 is expected to significantly affect the structure of the aggregate. If repulsive interactions dominate the free energy of the system will be minimised by reorganisation of surfactant molecules into a smaller number of larger aggregates. This would lead eventually to the formation of extensive bilayer in concentrated solution. In fact X-ray studies

[13,20] show that over the full nematic composition range the size of the micelle decreases with increasing volume fraction of amphiphile in such a way that the diameter is always of the order of separation of the centres of mass. On the other hand if the dominant interaction is attractive an explanation is required as to why the aggregates are not even smaller still, especially at low volume fractions of amphiphile.

Clearly, our present understanding of the factors which govern the structure and order of amphiphile aggregates in concentrated solutions is at a primitive level. Detailed experimental investigation of the effects of concentration and temperature on the size and shapes of the aggregates in the isotropic, nematic and lamellar and hexagonal phases of model systems are urgently required to remedy this situation.

(iv)Triple points and Krafft point.

The c.m.c's for both systems are of the same order (Cs^+ :- $1.9x10^{-2}$ mol kg^{-1}, NH_4^+ :- $2.5x10^{-2}$ mol kg^{-1}) as are the Krafft temperature (Cs^+ :- 279.0 K, NH_4^+ :- 279.2 K). Following micellation however the Tc curve for the ammonium salt is displaced to higher temperatures than that of the caesium salt as a consequence of the lower solubility of the ammonium salt.

Since higher concentrations are required for liquid crystal mesophases all triple points involving crystal plus liquid crystal phases (Tp(N,L,C) and Tp(I,N,C)) are displaced to higher temperature in the APFO/D_2O system. They also occur at much higher volume fractions. At Tp(I,N,C) the APFO volume fraction is 0.26 compared with the CsPFO volume fraction of 0.11 whilst the comparative figures for Tp(N,L,C)

are 0.30 and 0.14. The interaction parameter which is the driving force for the liquid crystal phase transition increases with volume fraction of amphiphile (equation 7) and decreases with increasing temperature so the increased volume fraction required for the APFO system may simply be a reflection of the higher temperature at which the the triple points occur.

The dependence of the pure liquid phase transition temperatures on volume fraction of amphiphile is shown in Fig 23. It is clear that over the full composition range for any given temperature $\Phi_A(NH_4^+)$ is greater than $\Phi_A(Cs^+)$. Assuming that equation 6 holds true for both these systems (i.e the interaction parameter, ε, depends only on T) this requires either a decrease in ε_{mm} or an increase in V_m (equation 7) A decrease in ε_{mm} is achieved by an decrease in the anisotropy of the micelle whilst an increase in V_m is of course associated with an increase in the aggregation number of the micelle. There could of course be a combination of both of these effects and resolution of this requires an extensive X-ray study over the full liquid crystal range.

Finally, Tp(CLN) may or may not be a true triple point depending on whether the lamellar to nematic transition is first or second order when it intersects with the solubility curve, Tc. If the transition is second order the nematic and lamellar phases are totally miscible and differ only in their symmetry elements so that they cannot be distinguished as separate phases. Again this problem awaits resolution.

Figure 23. Portions of the phase diagrams of the CsPFO/D_2O and APFO/D_2O systems showing the isotropic to nematic and nematic to lamellar phase transition lines. The composition scale is expressed as volume fraction amphiphile to facilitate interpretation of the differences in terms of equations 6 and 7.

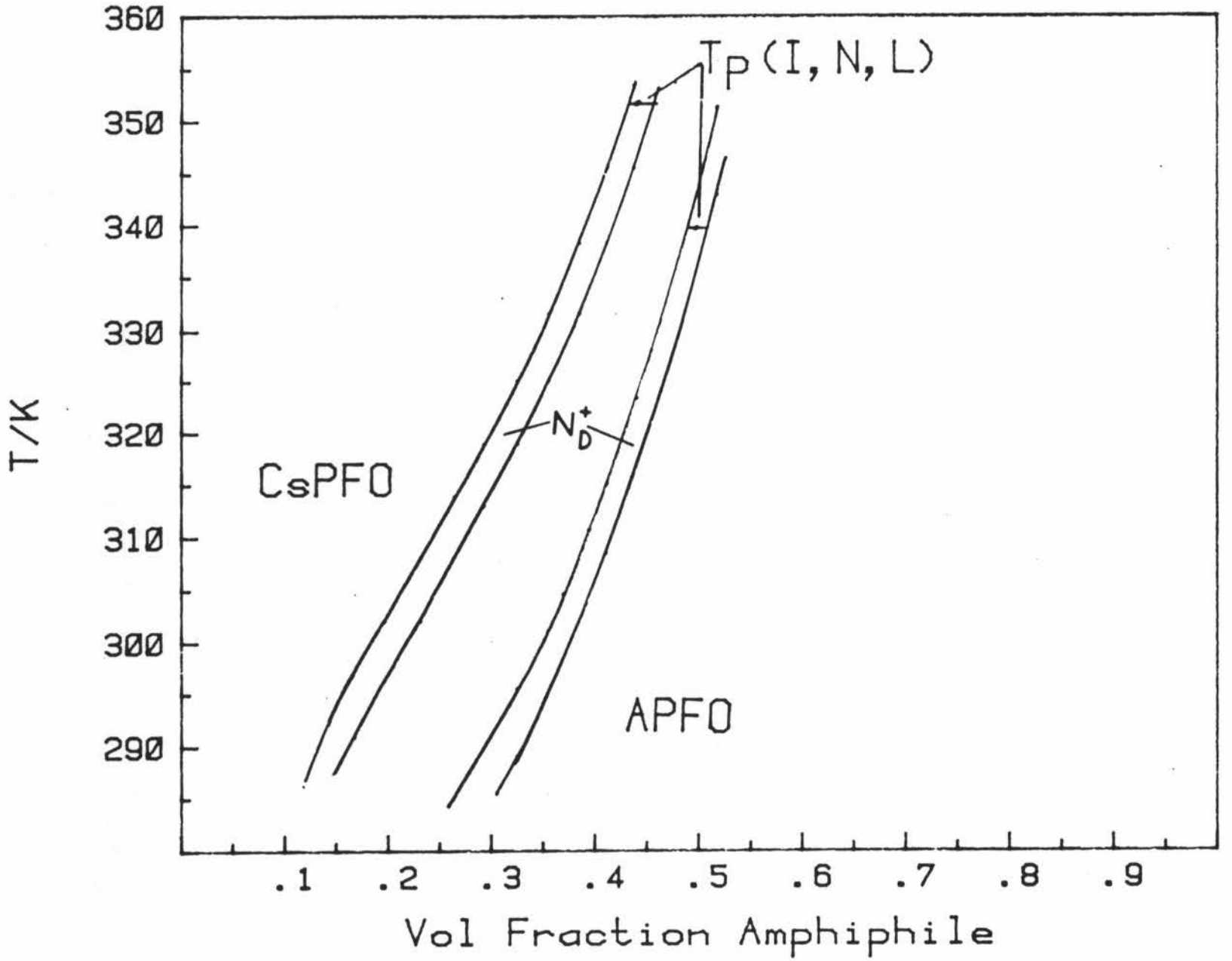
360
350
340
330
320
310
300
290
T/K
Tp (I, N, L)
N_D^+
CsPFO
APFO
.1
.2
.3
.4
.5
.6
.7
.8
.9
Vol Fraction Amphiphile

CONCLUSION

The phase diagrams of the CsPFO/D_2O and APFO/D_2O systems illustrate the wealth of information derivable about the fundamental physico-chemical properties of surfactant/water mixtures when such diagrams are mapped with high precision. The work presented in this thesis was the first stage of an investigation into the role of the counter-ion in determining the phase behaviour. Similarities in the two phase diagrams have been interpreted as being due to similarities in the structural unit which is a discoid micelle. Slight differences in the phase transition temperatures may be interpreted in terms of differing hydration enthalpies of the Cs^+ and NH_4^+ ions. Although phase diagrams for related systems have been reported [16] they are of poor quality and lack the precision to be of quantitative utility. Indeed some of the qualitative features of these diagrams are incorrect. To unravel the mysteries of the complex phenomena which are present in lyotropic amphiphilic liquid crystals reliable phase diagrams are required, not only for different counter-ions but also for different fluorocarbon (and hydrocarbon) moities. In particular, the construction of a high resolution phase diagram is an essential prerequisite to systematic studies of the mechanisms of phase transitions. Deuterium NMR is a method of exceptional utility in determining the nature of the phases present and in observing the changes which occur as two phase coexistence regions are transversed. For the first time the detailed changes on crossing these transitions have been interpreted in terms of exchange of D_2O between phases and new methods for measuring phase transition temperatures have been introduced. Finally and arguably, the most important factor when making physical measurements in these systems is precise control of temperature and concentration as

described in the main body of this thesis.

Bibliography

1. O Lehmann,
   Z. Krist., 18,464,(1890).

2. G Meier, in "Applications of Liquid Crystals",
   Springer-Verlag, Berlin Heidelberg, (1975).

3. S Chandrasekhar, "Liquid Crystals",
   Cambridge University Press, Cambridge, (1977).

4. G W Gray and J W Goodby, "Smectic Liquid Crystals",
   Leonard Hill, New York, (1984).

5. J Billard, in "Liquid Crystals of One- and Two-dimensional Order",
   (W Helfrich and G Heppke, Eds), Springer-Verlag,
   Berlin Heidelberg New York, (1980).

6. Encyclopedia Britannica.

7. P Ekwall, in "Advances in Liquid Crystals, Vol 1",
   (G H Brown, Ed), Academic Press, New York, (1975).

8. K D Lawson and T J Flautt,
   J. Am. Chem. Soc., 89, 5489, (1967).

9. N Boden, K Radley and M C Holmes,
   Mol. Phys., 42, 493, (1981).

10. J Charvolin,

Mol. Cryst. Liq. Cryst., 113, 1, (1984).

11. N Boden, S A Corne and K W Jolley,

Chem. Phys. Lett., 105, 99, (1984).

12. M C Holmes and J Charvolin,

J. Phys. Chem., 88, 810, (1984).

13. N Boden, S A Corne, M C Holmes, P H Jackson and K W Jolley,

J. de Physique, accepted for publication, (1986).

14. N Boden, P H Jackson, K McMullen and M C Holmes,

Chem. Phys. Lett., 65, 476, (1979).

15. N Boden, S A Corne and K W Jolley,

To be published J. Phys. Chem.

16. K Fontell and B Lindman,

J. Phys. Chem., 87, 3289, (1983).

17. H Hoffmann,

Ber. Bunsenges. Phys. Chem., 88, 1078, (1984).

18. K Reizlein and H Hoffmann,

Prog. in Colloid and Polymer Sci., 69, 83, (1984).

19. P Mukerjee, K Korematsu, M Okawauchi and G Sugihara,

J. Phys. Chem., 89, 5308, (1985).

20. N Boden and M C Holmes,
Chem. Phys. Lett., 100, 76, (1984).

21. W M Gelbart, A Ben-Shaul, W E McMullen and A Masters,
J. Phys. Chem., 88, 861, (1984).

22. G T J Tiddy,
Phys. Rep., 57, 7, (1980).

23. J Charvolin, A Levelut and E T Samulski,
J. Phys. (Paris) Lett., 40, L-587, (1979).

24. Y Hendrikx, J Charvolin, M Rawise, L Liebert and M C Holmes,
J. Phys. Chem., 87, 3991, (1983).

25. W Maier and A Saupe,
Z. Naturf. A , 14, 882, (1959);ibid, 15, 287, (1960).

26. C Rosenblatt, S Kumar and J D Litster,
Phys. Rev. A , 29, 1010, (1984).

27. B D Larson and J D Litster,
Mol. Cryst. Liq. Cryst., 113, 13, (1984).

28. W L McMillan,
Phys. Rev. A , 4, 1238, (1971); ibid, 6, 936, (1972).

29. N Boden and S A Jones,

Israel J. Chem., 23, 356, (1983).